LOW COMPLEXITY BLIND EQUALIZATION FOR SISO SYSTEMS WITH GENERAL CONSTELLATIONS

BY

ALA` AHMAD DAHMAN

A Thesis Presented to the
DEANSHIP OF GRADUATE STUDIES

KING FAHD UNIVERSITY OF PETROLEUM & MINERALS
DHAHRAN, SAUDI ARABIA

In Partial Fulfillment of the
Requirements for the Degree of

MASTER OF SCIENCE

In

TELECOMMUNICATION ENGINEERING

JUNE 2010

KING FAHD UNIVERSITY OF PETROLEUM & MINERALS
DHAHRAN 31261, SAUDI ARABIA

DEANSHIP OF GRADUATE STUDIES

This thesis, written by **ALA′ AHMAD DAHMAN** under the direction of his thesis adviser and approved by his thesis committee, has been presented to and accepted by the Dean of Graduate Studies, in partial fulfillment of the requirements for the degree of **MASTER OF SCIENCE IN TELECOMMUNICATION ENGINEERING**.

Thesis Committee

Dr. Tareq Y. Al-Naffouri (Advisor)

Azzedine Zerguine

Dr. Azzedine Zerguine (Member)

Dr. Samir Al-Ghadhban (Member)

(Member)

(Member)

Dr. Samir H. Abdul-Jauwad
Department Chairman

Dr. Salam Adel Zummo
Dean of Graduate Studies

3/8/10

Date

عمادة الدراسات العليا
DEANSHIP OF GRADUATE STUDIES

To My Parents,

My Wife

and My Daughters

ACKNOWLEDGMENTS

I reserve most thanks and appreciation to ALLAH the Almighty for His countless blessings and for enabling me to reach this stage of my studies. It is only He who drags me out of every problem I face. I pray that this work and the growth I had at KFUPM will be used in His cause.

I would like to thank King Fahd University of Petroleum & Minerals for giving me the opportunity to study and research at such a prestigious university.

It was a true honor to work with my advisor, Dr. Tareq Y. Al-Naffouri. I would like to take this opportunity to express my sincere gratitude and appreciation to him for the endless hours of guidance, ideas and support throughout my KFUPM experience. I have learned immensely from his deep knowledge, discipline, and intuition. Good guidance is very rare but I can easily rank his guidance as the best. It would not be an overstatement to say that he was surely the best teacher I ever had.

I would like to thank the members of my thesis committee, Dr. Azzedine Zerguine and Dr. Samir Al-Ghadhban for their assistance and valuable suggestions.

I would also like to thank Ahmed Abdul Quadeer and Muhammad S. Sohail for their support and guidance throughout my working on Thesis.

I was fortunate enough to have friends like Fouad, Anas, Raed, Mutaz, Farhat, Muhammad, Ahmad D., Ahmad S., Mahmoud, Sohaib, Abdullah, Rami, Isam, Bassel, Dia', Tamim, Ala', Shareef. It would be impossible for me to forget the time we spent together during playing games and visiting places. This work would not have been possible without their love, encouragement, motivation, and support.

Finally, I would like to thank my parents whose blessings and good wishes have brought me to this stage. It is very difficult to express my gratitude in words for their invaluable love and support. I would also like to thank my wife and my daughters (Dana and Layan) for their love, support, motivation, and patience during my stay at KFUPM. Thank you all.

TABLE OF CONTENTS

LIST OF TABLES **vii**

LIST OF FIGURES **viii**

ABSTRACT (ENGLISH) **x**

ABSTRACT (ARABIC) **xii**

CHAPTER 1 INTRODUCTION **1**

1.1 The Need for Channel Estimation in a Wireless Environment 2

1.2 Techniques for Channel Estimation and Data Detection 5

1.2.1 Constraints Used in Channel Estimation and Data Detection . . 5

1.2.2 Approaches to Channel Estimation and Data Detection 7

1.3 Overview of Contributions 9

1.3.1 Blind equalization for circular convolution SISO systems 9

1.3.2 Blind equalization for linear convolution SISO systems 10

1.3.3 Blind equalization for linear convolution SISO systems over time-variant channel 10

1.4 Notation 11

CHAPTER 2 BLIND EQUALIZATION FOR CIRCULAR CONVOLUTION SISO SYSTEMS **12**

2.1 Introduction 12

2.1.1 The Approach and Organization of the Chapter 14

2.2 System Overview . . . 15
2.2.1 Notation . . . 15
2.2.2 System Model . . . 16
2.2.3 Circular Convolution . . . 19
2.3 Blind Equalization Approach . . . 21
2.3.1 Exact Blind Algorithm . . . 26
2.3.2 Choice of the Initial Radius r . . . 28
2.4 Blind Equalization in the Constant Modulus Case . . . 29
2.5 Drawbacks of the Backtracking Algorithm . . . 29
2.6 Approximate Methods to Reduce the Computational Complexity Involved in Calculating $\boldsymbol{P}_i$ . . . 30
2.6.1 Avoiding $\boldsymbol{P}_i$ . . . 30
2.6.2 Avoiding $\boldsymbol{P}_i$ with Ordering $\boldsymbol{A}_i^*$ . . . 34
2.7 Minimum Cost Method . . . 37
2.8 Computational Complexity Comparison . . . 38
2.9 Simulation Results . . . 40
2.9.1 Blind Equalization . . . 41
2.9.2 Approximate Methods . . . 42
2.9.3 Enhanced Equalization Using Pilots . . . 45
2.10 Conclusion . . . 47
CHAPTER 3 BLIND EQUALIZATION FOR LINEAR CONVOLUTION SISO SYSTEMS 51
3.1 Introduction . . . 51
3.1.1 The Approach and Organization of the Chapter . . . 52
3.2 System Overview . . . 53
3.3 Blind Equalization Approach . . . 54
3.3.1 Exact Blind Algorithm . . . 58
3.4 Reducing the Computational Complexity . . . 59
3.5 Minimum Cost Method . . . 63

3.6 Computational Complexity Comparison 64
3.7 Simulation Results 65
3.7.1 Blind Equalization 65
3.7.2 Approximate Methods 66
3.8 Conclusion 69

CHAPTER 4 SISO SYSTEMS OVER TIME-VARIANT CHANNELS 73
4.1 Introduction 73
4.1.1 The Approach and Organization of this Chapter 74
4.2 Channel Model 75
4.3 Blind Equalization Approaches 77
4.3.1 Blind Equalization Without Knowledge of the Channel's Dynamical Model 78
4.3.2 Blind Equalization Using the Channel's Dynamical Model Information 80
4.4 Simulation Results 82
4.4.1 Performance of the three RLS algorithms 82
4.4.2 Effect of time variation 84
4.5 Conclusion 85

CHAPTER 5 CONCLUSIONS AND FUTURE WORK 88
5.1 Concluding Remarks 88
5.2 Future Work 90
5.2.1 General Time Variant Case for OFDM System 90
5.2.2 Motivating the Constant Modulus Algorithm 90
5.2.3 Enhancing the Minimum Cost Method 91
5.2.4 MIMO Channels Case 91

REFERENCES 92

VITAE 107

LIST OF TABLES

2.1 Estimated computational cost per iteration of the RLS algorithm . . . 39
2.2 Estimated computational cost per iteration of the RLS algorithm without calculating $\boldsymbol{P}_i$ 39
2.3 Computational cost comparison for OFDM blind algorithms 40
3.1 Computational cost comparison for SISO blind algorithms 65
4.1 Simulation and fading channel parameters 82

LIST OF FIGURES

2.1 Blind Algorithm Flowchart 28

2.2 Flowchart of the Minimum Cost Method 38

2.3 BER vs SNR for BPSK-OFDM over a Rayleigh channel 42

2.4 BER vs SNR for 4QAM-OFDM over a Rayleigh channel 43

2.5 BER vs SNR for 16QAM-OFDM over a Rayleigh channel 44

2.6 BER vs SNR for 4QAM-OFDM without using channel information 45

2.7 Comparison of low complexity algorithms for BPSK-OFDM 46

2.8 Comparison of low complexity algorithms for 4QAM-OFDM 47

2.9 Comparison of minimum cost method for BPSK-OFDM with $N = 64$ and $L = 15$ over a Rayleigh channel 48

2.10 Comparison of minimum cost method for 16QAM-OFDM with $N = 16$ and $L = 3$ over a Rayleigh channel 49

2.11 Comparison of minimum cost method for 16QAM-OFDM with $N = 64$ and $L = 7$ over a Rayleigh channel 49

2.12 BER vs SNR for BPSK-OFDM over a Rayleigh channel 50

2.13 BER vs SNR for 4QAM-OFDM over a Rayleigh channel 50

3.1 BER vs SNR for BPSK-SISO over a Rayleigh channel 66

3.2 BER vs SNR for 4QAM-SISO over a Rayleigh channel 67

3.3 BER vs SNR for 16QAM-SISO over a Rayleigh channel 68

3.4 Performance of low complexity algorithm for BPSK-SISO 69

3.5 Performance of low complexity algorithm for 4QAM-SISO 70

3.6 Performance of minimum cost method for BPSK-SISO over a Rayleigh channel 71

3.7 Performance of minimum cost method for 4QAM-SISO over a Rayleigh channel 71
3.8 Performance of minimum cost method for 16QAM-SISO over a Rayleigh channel 72

4.1 BER vs SNR for BPSK-SISO over time variant channel at low vehicle speed 83
4.2 BER vs SNR for BPSK-SISO over time variant channel at high vehicle speed 84
4.3 BER vs SNR for 4QAM-SISO over time variant channel at high vehicle speed 85
4.4 BER performance of EW-RLS method for BPSK over time variant channel . 86
4.5 BER performance of E-RLS method for BPSK over time variant channel . . 87
4.6 BER performance of F-RLS method for BPSK over time variant channel . . 87

THESIS ABSTRACT

NAME:	Ala′ Ahmad Dahman
TITLE OF STUDY:	Low Complexity Blind Equalization for SISO Systems with General Constellations
MAJOR FIELD:	Telecommunication Engineering
DATE OF DEGREE:	JUNE 2010

The demand for high data rate reliable communications poses great challenges to the next generation wireless systems in highly dynamic mobile environments. In this Thesis, we focus on the blind receiver design for SISO transmission over block fading and time-variant channels. We investigate the joint Maximum-Likelihood (ML) channel estimation and data detection for SISO wireless systems with general constellations and propose a low complexity blind algorithm for finding the exact joint ML solution. The method uses some a priori information about the communication problem to improve the channel estimation accuracy and bit error rate. The thesis considers two SISO systems; circular (OFDM systems) and linear convolution systems. In the circular convolution system, we show how an OFDM symbol, transmitted over block fading channel, can be blindly detected using the output symbols only. In the linear

convolution system, we perform a blind equalization for a data packet transmitted over block fading channel using the received symbols only. Finally, the thesis considers a more realistic problem in which we design a blind receiver for linear convolution SISO transmission over time-variant channels.

خلاصة الرساله

الاسم الكامل : علاء أحمد دهمان

عنوان الرساله : المساواه العمياء قليلة التعقيد لأنظمة القناه احادية المدخل والمخرج (SISO) لمجموعات النقاط (Constellations) العامه.

التخصص : هندسة الاتصالات

تاريخ الشهاده : يونيو 2010

الطلب على معدلات بث عالية للبيانات بشكل موثوق في أنظمة الاتصالات يفرض تحديات كبيره على الجيل القادم في الانظمه اللاسلكيه في بيئات كثيرة الحركه. في هذه الرساله تم التركيز على تصميم جهاز استقبال لانظمة SISO لقنوات متغيرة مع الزمن وقنوات ال block fading. استخدمنا الاحتماليه القصوى (Maximum Likelihood) المشتركه لتقدير قنوات البث والكشف عن المعلومات المرسله في أنظمة ال SISO اللاسلكيه لمجموعات النقاط (Constellations) العامه، واقتراح خوارزميه عمياء قليلة التعقيد لايجاد الاحتماليه القصوى المشتركه. هذه الطريقه تستخدم بعض المعلومات المسبقه عن نظام الاتصال لتحسين دقة التقدير وخفض معدل الاخطاء. الرساله تعتمد اثنين من انظمة ال SISO، الاول انظمة ال convolution الدائري (انظمة مضاعفة الانقسام الترددي المتعامد (OFDM))، والثاني انظمة ال convolution الخطي. في النظام الاول بيينا كيف ان رمز ال OFDM المرسل عبر قنوات ال block fading يمكن كشفه بشكل أعمى. اما في النظام الثاني فقد أجرينا مساواه عمياء لحزمة بيانات مرسله عبر قنوات ال block fading باستخدام الرمز المستقبل من القناه فقط. في الجزء الاخير من الرساله تم اعتماد نظام أكثر واقعيه حيث تم تصميم جهاز استقبال أعمى لأنظمة ال convolution الخطي المرسله عبر قنوات متغيره مع الزمن.

CHAPTER 1

INTRODUCTION

In a wireless system, data is sent over a time variant fading channel. At the receiver, we get the received signal convolved and corrupted with noise. Naturally we are interested in recovering the transmitted data. Suppose we have information about the channel over which the data is being transmitted. In this case, we can faithfully obtain the transmitted data by making use of the received signal and the channel information (through equalization). In reality, we do not have the prior knowledge of the transmission channel, and hence we have to settle for an estimate of the channel obtained at the receiver using some estimation technique. Channel estimation is thus an important step in receiver design. In a communication system, the sole purpose of the channel estimation is to recover the transmitted data.

The receiver in the wireless transmission systems must estimate the channel efficiently and subsequently the data in order to achieve high data rate. The receiver also needs to be of low complexity and should not require too much overhead. The problem becomes especially challenging in the wireless environment when the channel is time-variant. This Thesis is concerned with blind receivers for linear and circular convolution SISO systems over block fading and time-variant channels.

This introductory chapter sets the stage for the Thesis. It starts by discussing the need for channel estimation in Section 1.1. The chapter then presents an overview of the various channel estimation techniques that have been proposed in literature. We conclude the chapter by laying out the contributions of the subsequent chapters in Section 1.3 which also serve to outline the Thesis organization. In Section 1.4, we introduce our notation.

1.1 The Need for Channel Estimation in a Wireless Environment

In circular convolution SISO systems, a cyclic prefix (CP) is appended to the transmitted symbol. This allows OFDM to deal effectively with ISI by transforming the equalization problem into parallel single tap equalizers, while in linear convolution SISO systems, the equalization design becomes difficult because of the appearance of the ISI. In both cases, the equalizer taps need to be estimated in the wireless environment. These taps are usually time variant for a wireless channel. So it becomes essential for the receiver to estimate the channel continuously for proper data detection.

In the following, we summarize the major requirements in receiver design (channel estimation and data detection). The receiver needs to:

1. **Deal with time variant channels**

   The receiver needs to be able to deal with mobility, i.e. with time-variant channels. In doing so, the receiver needs to take care of the following constraints

   Reduce training overhead: The easiest way to deal with time-variant channels is to send enough pilots. Since, the channel impulse response (IR) can be as long as the CP of the OFDM symbol, which is roughly one-fourth the OFDM symbol length [5], each symbol would waste one-fourth of the throughput in training. Thus, the circular convolution SISO system receiver should employ more intelligent techniques for channel estimation that would avoid the need for excessive training and deal with time-variant channels.

   Avoid any latency by relying on the current symbol only: Some techniques for channel estimation might deal with the lack of enough training by relying on past or future symbols to perform some averaging-based channel estimation as is the case with many blind-based estimation techniques. This inherently assumes that the channel remains constant over several data packets which might not be true in a wireless scenario. Even if the channel is correlated from one packet to another, a filtering or smoothing approach to channel estimation requires excessive storage and results in undesirable latency.

   Thus, the proper answer to time-variant channels is to use as much natural structure as possible in the current data packet. This includes 1) The cyclic prefix in OFDM, 2) the finite alphabet constraint on the data, and 3) the channel finite delay spread and correlation, and rely as little as possible on smoothing or averaging techniques.

2. **Reduce complexity and storage requirements**

   As pointed out above, the algorithm should bootstrap itself from the current packet without need for storing past data and especially without having to rely on the future symbols. The bootstrap should not also come at the expense of increased complexity.

3. **Deal with special channel conditions**

   The receiver should be able to deal with some special channel conditions which include

   Time variation within the data packet: For applications with high mobility, the receiver should be able to deal with channels that vary within the data packet which gives rise to interference. However, a prerequisite for solving this problem is the ability to design a receiver that can cope with the milder block-fading variation problem [1].

   CP length shorter than the length of channel impulse response in OFDM: This is usually dealt with by using some channel impulse response shortening techniques.

[1]This Thesis focuses on the block fading model for OFDM system and both channel model (block fading and time-variant channels) for linear SISO system.

1.2 Techniques for Channel Estimation and Data Detection

As mentioned in the introduction, our aim is to design Blind algorithm for channel estimation and data detection. In this section, we will take a look at the literature relating to channel estimation and data detection. We will provide an overview of the various approaches to channel estimation and the different constraints assumed on channel and data.

The availability of an accurate channel transfer function estimate is one of the prerequisites for coherent symbol detection in the receiver. Numerous research contributions have appeared in literature on the topic of channel estimation, in recent years. One way to classify these works is as according to the method used for channel estimation (training based, semi blind, blind and data aided). Another approach to classify these algorithms is based on the constraints used for channel and data recovery.

1.2.1 Constraints Used in Channel Estimation and Data Detection

In literature, all algorithms for channel estimation use some inherent structure of the communication problem. This structure is produced by constraints on the data or the channel. In the following, we categorize the research work done on channel estimation on the basis of the constraints used.

Data Constraints

Finite alphabet constraint: Data is usually drawn from a finite alphabet [4], [34], [35], [57], [58].

Code: Data is coded before being transmitted which introduces redundancy and helps in reducing probability of error [27], [28], [31], [33], [47]-[50], [56].

Transmit precoding: Precoding might be done on the data at the transmitter to assist channel estimation at the receiver such as cyclic prefix in OFDM [4], [25], [30], [31], [40], [46], zero padding (silent guard bands) [8], [9], [10] and virtual carriers (the subcarriers that are set to zero without any information) [42], [43], [44], [63].

Pilots: Pilots i.e. training symbols for the receiver, have been extensively used for channel estimation [11]-[23].

Channel Constraints

Finite delay spread: The length of channel impulse response is considered to be finite and known to the receiver.

Frequency correlation: It is assumed that some additional statistical information about the channel taps is known. This is usually captured by the frequency correlation in the frequency response of the channel taps [4], [12], [31], [51], [59].

Time correlation: As channels vary with time, they show some form of time correlation. In a wireless environment, it is introduced by the doppler effect [4], [10],

[33], [52], [54].

1.2.2 Approaches to Channel Estimation and Data Detection

The algorithms used for channel estimation can also be divided on the basis of approach used. These approaches can be divided into four main categories.

Training based Estimation

Pilots i.e. symbols which are known to the receiver are sent with the data symbols so that the channel can be estimated and hence the data at the receiver (see [11]-[23]). Use of training sequences decreases the system bandwidth efficiency [24] and they are suitable only if the channel is assumed to be time-invariant. But as the wireless channel is time-varying, it becomes essential to transmit pilots periodically to keep track of the varying channel. Thus this further decreases the channel throughput.

Blind Estimation

The above limitations in training based estimation techniques motivated interest in the spectrally efficient blind approach. Only natural constraints are used for estimation in blind algorithms. For example, cyclic prefix and the cyclostationarity introduced by it was used by [25], [26], [29], [30], and [46] while coding was also used along with cyclic prefix by [31]. Redundant and non-redundant linear precoding was exploited in [27], [28], [33], [47]-[50] for channel estimation. Virtual carriers have also been used by [42]-[44] and constant modulus modulation was used by [45]. Receiver diversity was used in [36] while [37]-[41], [44] and the references therein developed a subspace approach using the second order statistics. The finite alphabet constraint on the data was explored by [34] and [35] and for reducing the computational complexity involved in it, adaptive techniques were explored by [32] and [33].

Semiblind Estimation

Semiblind techniques make use of both pilots and the natural constraints to efficiently estimate the channel. These methods use pilots to obtain an initial channel estimate and improve the estimate by using a variety of a priori information. Thus, in addition to the pilots, semiblind methods use the cyclic prefix [4], [31], [40], the finite alphabet constraint on the data as well as the frequency and time correlation of the channel [4], magnitude error in data [55], linear precoding [56], frequency correlation [12], [31], and [59], gaussian assumption on transmitted data [60], the first order statistics [61], subspace of the channel [62], receiver diversity and virtual carriers [63] for channel estimation and subsequent data detection. Semiblind adaptive approaches for channel estimation have also been exploited by [57] and [58] who in addition to pilots, utilized the finite alphabet nature of data and the second order statistics of the received signal, respectively.

Data-aided Estimation

The purpose of channel estimation is to use that estimate to detect data. The recovered data, in turn, can also be used to improve the channel estimate, thus giving rise to an iterative technique for channel and data recovery. This idea is the basis of joint channel estimation and data detection. This iterative technique was used in a data-aided fashion by [39] or more rigourously by the expectation maximization (EM) approach [68]-[73].

1.3 Overview of Contributions

1.3.1 Blind equalization for circular convolution SISO systems

In Chapter 2, we propose a totally blind algorithm for data detection by using the output observations only for circular convolution SISO systems (OFDM systems) employing data with general constellation. Our approach is based on [97] which proposed the joint Maximum-Likelihood (ML) channel estimation and signal detection problem for Single-Input Multiple-Output (SIMO) wireless systems. This algorithm rely on computing the cost function up to the time index i of the data symbols and compare it with an estimate value (radius) of the optimal solution of the cost function. We have extended this approach to OFDM system. In that chapter, we propose approximate methods to reduce the computational complexity involved in the new algorithm. A new pilot based estimation technique has also been proposed. Specifically, in this method, data is recovered by finding the constellation point that minimizing the cost function. As all standard-based OFDM systems involve some form of training, we have also studied the behavior of the blind receiver in the presence of pilots (training symbols).

1.3.2 Blind equalization for linear convolution SISO systems

In Chapter 3, we consider blind receiver design for linear convolution SISO transmission employing data with general constellation over block fading channels. The receiver employs the maximum likelihood (ML) algorithm for joint channel and data recovery, where the blind algorithm used in chapter 2 has been extended to linear convolution SISO systems. In that chapter, we also propose an approximate method to reduce the computational complexity involved in the blind algorithm where the Fast RLS algorithm has been utilized. A new equalization technique has also been proposed when the receiver has perfect or estimated knowledge of the channel. Specifically, in this method, data is recovered by finding the constellation point that minimizing the cost function.

1.3.3 Blind equalization for linear convolution SISO systems over time-variant channel

In Chapter 4, we solve a more realistic problem where we design a blind receiver for channel estimation and data recovery for linear convolution SISO transmission over time-variant channels. The receiver uses some possible constraints on the channel (the finite delay spread and frequency and time correlation) and the data (the finite alphabet constraint). Our approach is based on [97] which proposed the joint ML channel estimation and signal detection problem for SIMO wireless systems over block fading channel. We have extended this approach to SISO transmission over time-variant channel. Three modification/extensions of the RLS algorithm were employed by the new blind algorithm to track the channel and time diversity which include the exponentially weighted RLS, the Fast RLS and the Extended RLS algorithm. We have also discussed the effect of the time variation parameters on the performance of the receiver.

1.4 Notation

We summarize here our notational guidelines for ease of reference. We denote scalars with small-case letters (e.g. x), vectors with small-case boldface letters (e.g. $\boldsymbol{x}$), and matrices with uppercase boldface letters (e.g. $\boldsymbol{X}$). Calligraphic notation (e.g. $\boldsymbol{\mathcal{X}}$) is reserved for vectors in the frequency domain. The individual entries of a vector like $\boldsymbol{h}$ are denoted by $h(l)$. A hat over a variable indicates an estimate of the variable (e.g., $\hat{\boldsymbol{h}}$ is an estimate of $\boldsymbol{h}$). When any of these variables become a function of time, the time index i appears as a subscript. We use the superscript $*$ to denote transposition with complex conjugation.

CHAPTER 2

BLIND EQUALIZATION FOR CIRCULAR CONVOLUTION SISO SYSTEMS

2.1 Introduction

The motive of modern broadband wireless communication systems is to offer high data rate services. The main hindrance for such high data rate systems is multipath fading as it results in inter-symbol interference (ISI). It therefore becomes essential to use such modulation techniques that are robust to multipath fading. Multicarrier techniques especially Orthogonal Frequency Division Multiplexing (OFDM) has emerged as a modulation scheme that can achieve high data rate by efficiently handling multipath effects. The additional advantages of simple implementation and high spectral efficiency due to orthogonality contribute towards the increasing interest in

OFDM. This is reflected by the many standards that considered and adopted OFDM, including those for digital audio and video broadcasting (DAB and DVB), WIMAX (Worldwide Interoperability for Microwave Access), high speed modems over digital subscriber lines, and local area wireless broadband standards such as the HIPERLAN/2 and IEEE 802.11a, with data rates of up to 54 Mbps [1]. OFDM is also being considered for fourth-generation (4G) mobile wireless systems [2].

In order to achieve high data rate in OFDM, the receivers must be well designed i.e. it must estimate the channel efficiently and subsequently the data. The receiver also needs to be of low complexity and should not require too much overhead. The problem becomes especially challenging in the wireless environment when the channel is time-variant. Several blind channel estimation algorithms have been devised for OFDM systems. Some of them are based on a subspace approach exploiting the cyclostationary property that is inherent to OFDM transmissions in the cyclic prefix [100] [26]. Another type of blind channel estimator capitalizes on the finite alphabet property of the modulated symbols [39]. Many other techniques have been proposed in the literature for this purpose too (see, e.g., [1], [4], [99], [98]).

In this chapter, we propose a low complexity algorithm for blind equalization in circular convolution SISO systems (OFDM systems) employing data with general constellations. The algorithm is able to recover the data from the output observations only. This is done for one OFDM symbol allowing the algorithm to work in block fading channels.

2.1.1 The Approach and Organization of the Chapter

This chapter proposes a blind receiver for the OFDM systems by using a new algorithm, which showed a favorable performance whether operating in the blind or training modes.

In the first part of the chapter, we perform data estimation and equalization from output observations only, without the need for a training sequence or a priori channel information. The advantage of our approach is three fold:

1. The method provides a *blind estimate* of the data from one output symbol without the need for training. Thus, the method lends itself to block fading channels.

2. The algorithm works on OFDM systems employing data with *general constellations*.

3. Data equalization is done *without* any restriction on the channel

We start with setup the OFDM system model in Section 2.2. Our approach is based on joint maximum-likelihood (ML) channel estimation and signal detection problem for OFDM wireless systems with general modulation constellations and propose an efficient algorithm for finding the exact joint ML solution (see Section 2.3). The algorithm takes a particularly simple form in constant modulus case (see Section 2.4).

The new blind algorithm can be computationally expensive with two drawbacks explained in Section 2.5. We thus suggest in the second part of the chapter (Sections 2.6 and 2.7), three approaches to reduce this computational complexity. In the first and second approaches, we try to simplify the new algorithm by avoiding the need of calculating one of its big matrices. In the third approach, we propose a very low complexity method to detect the data based on the minimum cost. These three methods have different complexity, thus we compare their computational complexity in Section 2.8. Simulation results are discussed in Section 2.9 with conclusion in Section 2.10.

2.2 System Overview

2.2.1 Notation

Consider a length-N vector $\boldsymbol{x}_i$. We deal with three derivatives associated with this vector. The first two are obtained by partitioning $\boldsymbol{x}_i$ into a lower (trailing) part $\underline{\boldsymbol{x}}_i$ (known as the cyclic prefix) and an upper vector $\tilde{\boldsymbol{x}}_i$ so that

$$\boldsymbol{x}_i = \begin{bmatrix} \tilde{\boldsymbol{x}}_i \\ \underline{\boldsymbol{x}}_i \end{bmatrix}$$

The third derivative, $\overline{\boldsymbol{x}}_i$, is created by concatenating $\boldsymbol{x}_i$ with a copy of CP i.e. $\underline{\boldsymbol{x}}_i$. Thus, we have

$$\overline{\boldsymbol{x}}_i = \begin{bmatrix} \underline{\boldsymbol{x}}_i \\ \boldsymbol{x}_i \end{bmatrix} = \begin{bmatrix} \underline{\boldsymbol{x}}_i \\ \tilde{\boldsymbol{x}}_i \\ \underline{\boldsymbol{x}}_i \end{bmatrix} \tag{2.1}$$

In line with the above notation, a matrix $\boldsymbol{Q}$ having N rows will have the natural partitioning

$$\boldsymbol{Q} = \begin{bmatrix} \tilde{\boldsymbol{Q}} \\ \underline{\boldsymbol{Q}} \end{bmatrix} \tag{2.2}$$

where the number of rows in $\tilde{\boldsymbol{Q}}$ and $\underline{\boldsymbol{Q}}$ are understood from the context and when it is not clear, the number of rows will appear as a subscript.Thus, we write

$$\boldsymbol{Q} = \begin{bmatrix} \tilde{\boldsymbol{Q}}_{N-L} \\ \underline{\boldsymbol{Q}}_L \end{bmatrix} \tag{2.3}$$

2.2.2 System Model

In an OFDM system, data is transmitted in symbols $\boldsymbol{\mathcal{X}}_i$ of length N each. The symbol undergoes an IFFT operation to produce the time domain symbol $\boldsymbol{x}_i$, i.e.

$$\boldsymbol{x}_i = \sqrt{N}\boldsymbol{Q}\boldsymbol{\mathcal{X}}_i \tag{2.4}$$

where $\boldsymbol{Q}$ is the $N \times N$ IFFT matrix. When juxtaposed, these symbols result in the sequence $\{x_k\}$. [1] We assume a channel $\underline{\boldsymbol{h}}$ of maximum length $L+1$. To avoid ISI caused by passing through the channel, a cyclic prefix (CP) $\underline{\boldsymbol{x}}_i$ (of length L) is appended to $\boldsymbol{x}_i$, resulting in super-symbol $\overline{\boldsymbol{x}}_i$ as defined in (2.1). The concatenation of these symbols produces the underlying sequence $\{\overline{x}_k\}$. When passed through the

[1] The time indices in the sequence $\boldsymbol{x}_i$ and the underlying sequence $\{x_k\}$ are dummy variables. Nevertheless, we chose to index the two sequences differently to avoid any confusion that might arise from choosing identical indices.

channel $\underline{\boldsymbol{h}}$, the sequence $\{\overline{x}_k\}$ produces the output sequence $\{\overline{y}_k\}$ i.e.

$$\overline{y}_k = \underline{h}_k * \overline{x}_k + \overline{n}_k \tag{2.5}$$

where $\overline{n}_k$ is the additive white Gaussian noise and $*$ stands for linear convolution. Motivated by the symbol structure of the input, it is convenient to partition the output into length $N + L$ symbol as

$$\overline{\boldsymbol{y}}_i = \begin{bmatrix} \underline{\boldsymbol{y}}_i \\ \boldsymbol{y}_i \end{bmatrix}$$

This is a natural way to partition the output because the prefix $\underline{\boldsymbol{y}}_i$ actually absorbs all ISI that takes place between the adjacent symbols $\overline{\boldsymbol{x}}_{i-1}$ and $\overline{\boldsymbol{x}}_i$. Moreover, the remaining part $\boldsymbol{y}_i$ of the symbol depends on the ith input OFDM symbol $\boldsymbol{x}_i$ only. These facts can be seen from the input/output relationship

$$\begin{bmatrix} \boldsymbol{y}_{i-1} \\ \underline{\boldsymbol{y}}_i \\ \boldsymbol{y}_i \end{bmatrix} = \begin{bmatrix} \overline{\boldsymbol{H}} & & \boldsymbol{O}_{N\times L} & \boldsymbol{O}_{N\times N} \\ \boldsymbol{O}_{L\times N} & \underline{\boldsymbol{H}}_U & \underline{\boldsymbol{H}}_L & \boldsymbol{O}_{L\times N} \\ \boldsymbol{O}_{N\times N} & \boldsymbol{O}_{N\times L} & \overline{\boldsymbol{H}} & \end{bmatrix} \begin{bmatrix} \underline{\boldsymbol{x}}_{i-1} \\ \tilde{\boldsymbol{x}}_{i-1} \\ \underline{\boldsymbol{x}}_{i-1} \\ \underline{\boldsymbol{x}}_i \\ \tilde{\boldsymbol{x}}_i \\ \underline{\boldsymbol{x}}_i \end{bmatrix} + \begin{bmatrix} \boldsymbol{n}_{i-1} \\ \underline{\boldsymbol{n}}_i \\ \boldsymbol{n}_i \end{bmatrix} \tag{2.6}$$

where $\boldsymbol{n}$ is the output noise which we take to be white Gaussian. The matrices $\overline{\boldsymbol{H}}$, $\underline{\boldsymbol{H}}_{\mathsf{L}}$, and $\underline{\boldsymbol{H}}_{\mathsf{U}}$ are convolution (Toeplitz) matrices of proper sizes created from the vector $\underline{\boldsymbol{h}}$. Specifically, $\overline{\boldsymbol{H}}$ is the $N \times (N + L)$ matrix

$$\overline{\boldsymbol{H}} = \begin{bmatrix} \underline{h}(L) & \cdots & \underline{h}(1) & \underline{h}(0) & & \\ \vdots & \ddots & \cdots & \ddots & \ddots & \\ 0 & \cdots & \underline{h}(L) & \cdots & \underline{h}(1) & \underline{h}(0) \end{bmatrix} \tag{2.7}$$

The matrices $\underline{\boldsymbol{H}}_{\mathsf{U}}$ and $\underline{\boldsymbol{H}}_{\mathsf{L}}$ are square of size L.[2]

$$\underline{\boldsymbol{H}}_{\mathsf{U}} = \begin{bmatrix} \underline{h}(L) & \underline{h}(L-1) & \cdots & \underline{h}(1) \\ & \underline{h}(L) & \cdots & \underline{h}(2) \\ & & \ddots & \vdots \\ & & & \underline{h}(L) \end{bmatrix} \tag{2.8}$$

$$\underline{\boldsymbol{H}}_{\mathsf{L}} = \begin{bmatrix} \underline{h}(0) & & & \\ \underline{h}(1) & \underline{h}(0) & & \\ \vdots & \ddots & \ddots & \\ \underline{h}(L-1) & \cdots & \underline{h}(1) & \underline{h}(0) \end{bmatrix} \tag{2.9}$$

[2]The matrix $\underline{\boldsymbol{H}}_{\mathsf{L}}$ ($\underline{\boldsymbol{H}}_{\mathsf{U}}$) is lower (upper) triangular; this explains the superscript L (U).

2.2.3 Circular Convolution

From (2.6), we can write

$$\boldsymbol{y}_i = \overline{\boldsymbol{H}} \begin{bmatrix} \underline{\boldsymbol{x}}_i \\ \tilde{\boldsymbol{x}}_i \\ \underline{\boldsymbol{x}}_i \end{bmatrix} = \overline{\boldsymbol{H}}\, \overline{\boldsymbol{x}}_i + \boldsymbol{n}_i \tag{2.10}$$

This shows that $\boldsymbol{y}_i$ is created solely from $\overline{\boldsymbol{x}}_i$ through convolution and hence is ISI-free. Moreover, the existence of a cyclic prefix in $\overline{\boldsymbol{x}}_i$ allows us to rewrite (2.10) as

$$\boldsymbol{y}_i = \boldsymbol{H}\boldsymbol{x}_i + \boldsymbol{n}_i \tag{2.11}$$

where $\boldsymbol{H}$ is the size-N circulant matrix.

$$\boldsymbol{H} = \begin{bmatrix} \underline{h}(0) & 0 & \cdots & 0 & \underline{h}(L) & \cdots & \underline{h}(1) \\ \underline{h}(1) & \underline{h}(0) & \cdots & 0 & 0 & \cdots & \underline{h}(2) \\ \vdots & \vdots & \ddots & \vdots & \cdots & \ddots & \vdots \\ \underline{h}(L) & \underline{h}(L-1) & \cdots & \underline{h}(0) & 0 & \cdots & 0 \\ \vdots & \ddots & \ddots & \cdots & \ddots & \vdots & \vdots \\ 0 & 0 & \cdots & \underline{h}(L) & \underline{h}(L-1) & \cdots & \underline{h}(0) \end{bmatrix} \tag{2.12}$$

In other words, the cyclic prefix of $\overline{\boldsymbol{x}}_i$ renders the convolution in (2.11) cyclic, and we can write

$$\boxed{\boldsymbol{y}_i = \boldsymbol{h}_i \circledast \boldsymbol{x}_i + \boldsymbol{n}_i} \tag{2.13}$$

where $\circledast$ is the circular convolution, and $\boldsymbol{h}_i$ is a length-N zero-padded version of $\underline{\boldsymbol{h}}_i$.

$$\boldsymbol{h}_i = \begin{bmatrix} \underline{\boldsymbol{h}}_i \\ \boldsymbol{O}_{(N-L-1)\times 1} \end{bmatrix}$$

In the frequency domain, the circular convolution (2.13) reduces to the element-by-element operation

$$\boxed{\boldsymbol{\mathcal{Y}}_i = \boldsymbol{\mathcal{H}}_i \odot \boldsymbol{\mathcal{X}}_i + \boldsymbol{\mathcal{N}}_i} \qquad (2.14)$$

where $\odot$ stands for element-by-element multiplication and where $\boldsymbol{\mathcal{H}}_i$, $\boldsymbol{\mathcal{X}}_i$, $\boldsymbol{\mathcal{N}}_i$, and $\boldsymbol{\mathcal{Y}}_i$, are the DFT's of $\boldsymbol{h}_i$, $\boldsymbol{x}_i$, $\boldsymbol{n}_i$, and $\boldsymbol{y}_i$ respectively

$$\boldsymbol{\mathcal{H}}_i = \boldsymbol{Q}^*\boldsymbol{h}_i, \quad \boldsymbol{\mathcal{X}}_i = \frac{1}{\sqrt{N}}\boldsymbol{Q}^*\boldsymbol{x}_i, \quad \boldsymbol{\mathcal{N}}_i = \frac{1}{\sqrt{N}}\boldsymbol{Q}^*\boldsymbol{n}_i, \text{ and } \boldsymbol{\mathcal{Y}}_i = \frac{1}{\sqrt{N}}\boldsymbol{Q}^*\boldsymbol{y}_i \qquad (2.15)$$

Since $\underline{\boldsymbol{h}}_i$ corresponds to the first $L+1$ elements of $\boldsymbol{h}_i$, we can show that

$$\boldsymbol{\mathcal{H}}_i = \boldsymbol{A}^*\underline{\boldsymbol{h}}_i \quad \text{and} \quad \underline{\boldsymbol{h}}_i = \boldsymbol{A}\boldsymbol{\mathcal{H}}_i \qquad (2.16)$$

where $\boldsymbol{A}^*$ consists of the first $L+1$ columns of $\boldsymbol{Q}^*$ and $\boldsymbol{A}$ consists of first $L+1$ rows of $\boldsymbol{Q}$. This allows us to rewrite (2.14) as

$$\boxed{\boldsymbol{\mathcal{Y}}_i = \mathrm{diag}(\boldsymbol{\mathcal{X}}_i)\boldsymbol{A}^*\underline{\boldsymbol{h}}_i + \boldsymbol{\mathcal{N}}_i} \qquad (2.17)$$

2.3 Blind Equalization Approach

Consider input/outout equation (2.14), reproduced here for convenience

$$\boldsymbol{\mathcal{Y}} = \boldsymbol{\mathcal{H}} \odot \boldsymbol{\mathcal{X}} + \boldsymbol{\mathcal{N}} \tag{2.18}$$

$$= \text{diag}(\boldsymbol{\mathcal{X}})\boldsymbol{\mathcal{H}} + \boldsymbol{\mathcal{N}} \tag{2.19}$$

Element by element, this equation can be written as

$$\mathcal{Y}(j) = \mathcal{X}(j)\mathcal{H}(j) + \mathcal{N}(j)$$

or since $\boldsymbol{\mathcal{H}} = \boldsymbol{A}^*\underline{\boldsymbol{h}}$,

$$\mathcal{Y}(j) = \mathcal{X}(j)\boldsymbol{a}_j^*\underline{\boldsymbol{h}} + \mathcal{N}(j)$$

where $\boldsymbol{a}_j^*$ is the jth row of $\boldsymbol{A}^*$ (so that $\boldsymbol{a}_j$ is the jth column of $\boldsymbol{A}$).

The problem of joint ML channel estimation and data detection for OFDM channels is transformed into the following minimization problem

$$J = \min_{h,\mathcal{X}\in\Omega^N} \|\boldsymbol{\mathcal{Y}} - \text{diag}(\boldsymbol{\mathcal{X}})\boldsymbol{A}^*\underline{\boldsymbol{h}}\|^2 \tag{2.20}$$

$$= \min_{h,\mathcal{X}\in\Omega^N} \sum_{i=1}^{N} |\mathcal{Y}(i) - \mathcal{X}(i)\boldsymbol{a}_i^*\underline{\boldsymbol{h}}|^2 \tag{2.21}$$

$$= \min_{h,\mathcal{X}\in\Omega^N} \sum_{j=1}^{i} |\mathcal{Y}(j) - \mathcal{X}(j)\boldsymbol{a}_j^*\underline{\boldsymbol{h}}|^2 + \sum_{j=i+1}^{N} |\mathcal{Y}(j) - \mathcal{X}(j)\boldsymbol{a}_j^*\underline{\boldsymbol{h}}|^2 \tag{2.22}$$

where Ω^N denotes the set of $N-$dimensional signal vector.

Let us consider a partial data sequence $\boldsymbol{\mathcal{X}}_{(i)}$ up to the time index i i.e.

$$\boldsymbol{\mathcal{X}}_{(i)} = [\mathcal{X}(1) \;\; \mathcal{X}(2) \;\; \cdots \;\; \mathcal{X}(i)]$$

and define $M_{\mathcal{X}_{(i)}}$ as the cost function of the first i data symbols, say

$$M_{\mathcal{X}_{(i)}} = \|\boldsymbol{\mathcal{Y}}_{(i)} - \text{diag}(\boldsymbol{\mathcal{X}}_{(i)})\boldsymbol{A}^*_{(i)}\underline{\boldsymbol{h}}\|^2 \tag{2.23}$$

where $\boldsymbol{A}^*_{(i)}$ consists of the first i rows of $\boldsymbol{A}^*$.

Now, as per Weiyu's paper [97], let R be the optimal value for our objective function in (2.20), if $M_{\mathcal{X}_{(i)}} > R$, then $\boldsymbol{\mathcal{X}}_{(i)}$ can not be the first i symbols of the ML solution $\hat{\boldsymbol{\mathcal{X}}}_{(i)}$ to (2.20). To prove this, suppose $\boldsymbol{\mathcal{X}}_{(i)} = \hat{\boldsymbol{\mathcal{X}}}_{(i)}$ and we denote the optimal channel gains corresponding to $\hat{\boldsymbol{\mathcal{X}}}_{(i)}$ as $\hat{\underline{\boldsymbol{h}}}$. Then

$$\begin{aligned}
R &= \|\boldsymbol{\mathcal{Y}}_{(i)} - \text{diag}(\hat{\boldsymbol{\mathcal{X}}}_{(i)})\boldsymbol{A}^*_{(i)}\hat{\underline{\boldsymbol{h}}}\|^2 + \sum_{j=i+1}^{N} |\mathcal{Y}(j) - \hat{\mathcal{X}}(j)\boldsymbol{a}_j^*\hat{\underline{\boldsymbol{h}}}|^2 && (2.24)\\
&\geq \min_{h} \|\boldsymbol{\mathcal{Y}}_{(i)} - \text{diag}(\hat{\boldsymbol{\mathcal{X}}}_{(i)})\boldsymbol{A}^*_{(i)}\underline{\boldsymbol{h}}\|^2 + \sum_{j=i+1}^{N} |\mathcal{Y}(j) - \hat{\mathcal{X}}(j)\boldsymbol{a}_j^*\hat{\underline{\boldsymbol{h}}}|^2 && (2.25)\\
&\geq \min_{h} \|\boldsymbol{\mathcal{Y}}_{(i)} - \text{diag}(\hat{\boldsymbol{\mathcal{X}}}_{(i)})\boldsymbol{A}^*_{(i)}\underline{\boldsymbol{h}}\|^2 = M_{\hat{\mathcal{X}}_{(i)}} = M_{\mathcal{X}_{(i)}} && (2.26)
\end{aligned}$$

So, for $\boldsymbol{\mathcal{X}}_{(i)}$ to correspond to the first i symbols of the ML solution $\hat{\boldsymbol{\mathcal{X}}}_{(i)}$, we should have $M_{\mathcal{X}_{(i)}} < R$. Note that the above represents a necessary condition only in that if $\hat{\boldsymbol{\mathcal{X}}}_{(i)}$ is such that $M_{\mathcal{X}_{(i)}} < R$, then that does not necessarily mean that $\hat{\boldsymbol{\mathcal{X}}}_{(i)}$ coincides with $\boldsymbol{\mathcal{X}}_{(i)}$. In the next subsection (2.3.1), we will use this properly in our blind algorithm.

Since $\boldsymbol{A}^*_{(i)}$ is full rank for $i \leq L+1$, $\text{diag}(\boldsymbol{\mathcal{X}}_{(i)})\boldsymbol{A}^*_{(i)}$ is full rank too for each choice of $\text{diag}(\boldsymbol{\mathcal{X}}_{(i)})$ and so we will always find some $\underline{\boldsymbol{h}}$ that will make the first part of the objective function zero (since $\underline{\boldsymbol{h}}$ has exactly $L+1$ degrees of freedom). Thus, our search tree should be at least of depth $L+1$. This explains why $L+1$ pilots are needed in OFDM. To reduce the search space, we could use p pilots ($p < L+1$) and hence need only deal with a tree of depth $L+1-p$ (without loss of generality, we can place all pilots at the beginning of the symbol $\boldsymbol{\mathcal{X}}$).

Assuming that we have some initial guess, let's see how we can update the objective function when we move down the tree by one level. The objective function can be updated according to some recursion. Specifically, assume that we obtained the cost function involved in minimizing

$$M_{\mathcal{X}_{(i-1)}} = \|\boldsymbol{\mathcal{Y}}_{(i)} - \text{diag}(\boldsymbol{\mathcal{X}}_{(i)})\boldsymbol{A}^*_{(i)}\underline{\boldsymbol{h}}\|^2$$

and we would like to obtain the cost function for the next iteration. From the above discussion, we know that $M_{\mathcal{X}_{(i)}} = 0$ for $i \leq L+1$. For $i > L+1$, the cost can be obtained using Recursive Least Squares (RLS) algorithm [92] by the following set of iterations

$$M_{\mathcal{X}_{(i)}} = M_{\mathcal{X}_{(i-1)}} + \gamma(i)|\mathcal{Y}(i) - \mathcal{X}(i)\boldsymbol{a}_i^*\hat{\underline{\boldsymbol{h}}}_{i-1}|^2 \quad (2.27)$$

$$\hat{\underline{\boldsymbol{h}}}_i = \hat{\underline{\boldsymbol{h}}}_{i-1} + \boldsymbol{g}_i(\mathcal{Y}(i) - \mathcal{X}(i)\boldsymbol{a}_i^*\hat{\underline{\boldsymbol{h}}}_{i-1}) \quad (2.28)$$

where

$$\boldsymbol{g}_i = \gamma(i)\mathcal{X}^*(i)\boldsymbol{P}_{i-1}\boldsymbol{a}_i \tag{2.29}$$

$$\gamma(i) = \frac{1}{1+|\mathcal{X}(i)|^2\boldsymbol{a}_i^*\boldsymbol{P}_{i-1}\boldsymbol{a}_i} \tag{2.30}$$

$$\boldsymbol{P}_i = \boldsymbol{P}_{i-1} - \gamma(i)|\mathcal{X}(i)|^2\boldsymbol{P}_{i-1}\boldsymbol{a}_i\boldsymbol{a}_i^*\boldsymbol{P}_{i-1} \tag{2.31}$$

The recursions are initialized by

$$M_{\mathcal{X}_{(L+1)}} = 0, \quad \boldsymbol{P}_{L+1} = \left(\boldsymbol{A}_{(L+1)}\text{diag}(|\boldsymbol{\mathcal{X}}_{(i)}|^2)\boldsymbol{Q}^*_{(L+1)}\right)^{-1},$$

$$\text{and} \quad \underline{\hat{\boldsymbol{h}}}_{L+1} = \boldsymbol{P}_{L+1}\boldsymbol{A}_{(L+1)}\text{diag}(\boldsymbol{\mathcal{X}}^*_{(i)})\boldsymbol{\mathcal{Y}}_{(i)}$$

Now since $\underline{\boldsymbol{h}}$ has $L+1$ degrees of freedom, we need $L+1$ pilots to identify it, or alternatively, we need to guess $L+1$ solutions before we can move on. The reason is that $\underline{\boldsymbol{h}}$ has $L+1$ degrees of freedom.

We could also calculate the cost function without obtaining the actual value of the solution $\underline{\boldsymbol{h}}_i$ using the recursion

$$M_{\mathcal{X}_{(i)}} = \boldsymbol{\mathcal{Y}}^*_{(i)}\left(\boldsymbol{I} - \text{diag}(\boldsymbol{\mathcal{X}}_{(i)})\boldsymbol{A}^*_{(i)}\boldsymbol{P}_i\boldsymbol{A}_{(i)}\text{diag}(\boldsymbol{\mathcal{X}}^*_{(i)})\right)^{-1}\boldsymbol{\mathcal{Y}}_{(i)} \tag{2.32}$$

with $\boldsymbol{P}_i$ calculated recursively as in above. However, this solution is computationally more complex than the RLS solution above.

The problem with the above approach is that we need to have the value of $L+1$ $\boldsymbol{\mathcal{X}}(i)'$s before starting to have a nonzero value for the objective function. An alternative strategy would be to find $\underline{\boldsymbol{h}}$ using weighted regularized least squares. Specifically, instead of minimizing the objective function J in equation (2.20), we minimize

$$J = \min_{h,\mathcal{X}\in\Omega^N} \|\underline{\boldsymbol{h}}\|^2_{R_h^{-1}} + \|\boldsymbol{\mathcal{Y}} - \text{diag}(\boldsymbol{\mathcal{X}})\boldsymbol{A}^*\underline{\boldsymbol{h}}\|^2_{R_n^{-1}} \tag{2.33}$$

$$= \min_{h,\mathcal{X}\in\Omega^N} \|\underline{\boldsymbol{h}}\|^2_{R_h^{-1}} + \frac{1}{\sigma^2}\sum_{i=1}^{N} |\mathcal{Y}(i) - \mathcal{X}(i)\boldsymbol{a}_i^*\underline{\boldsymbol{h}}|^2 \tag{2.34}$$

where $\boldsymbol{R}_h$ is some weighting matrix that could be taken as the autocorrelation matrix of $\underline{\boldsymbol{h}}$ and $\boldsymbol{R}_n$ is the autocorrelation matrix of the noise given by $\sigma^2\boldsymbol{I}$, where σ^2 is the noise variance. With this modification, we can recursively calculate the value of the objective function for each i through the following set of recursions similar to the ones we have above, and we called it through this chapter as *Blind RLS Algorithm*:

$$\boxed{M_{\mathcal{X}_{(i)}} = M_{\mathcal{X}_{(i-1)}} + \tfrac{1}{\sigma^2}\gamma(i)|\mathcal{Y}(i) - \mathcal{X}(i)\boldsymbol{a}_i^*\hat{\underline{\boldsymbol{h}}}_{i-1}|^2} \tag{2.35}$$

$$\boxed{\hat{\underline{\boldsymbol{h}}}_i = \hat{\underline{\boldsymbol{h}}}_{i-1} + \tfrac{1}{\sigma}\boldsymbol{g}_i\left(\mathcal{Y}(i) - \mathcal{X}(i)\boldsymbol{a}_i^*\hat{\underline{\boldsymbol{h}}}_{i-1}\right)} \tag{2.36}$$

where

$$\boldsymbol{g}_i = \frac{1}{\sigma}\gamma(i)\mathcal{X}(i)^*\boldsymbol{P}_{i-1}\boldsymbol{a}_i \tag{2.37}$$

$$\gamma(i) = \frac{1}{1 + \frac{1}{\sigma^2}|\mathcal{X}(i)|^2\boldsymbol{a}_i^*\boldsymbol{P}_{i-1}\boldsymbol{a}_i} \tag{2.38}$$

$$\boldsymbol{P}_i = \boldsymbol{P}_{i-1} - \frac{1}{\sigma^2}\gamma(i)|\mathcal{X}(i)|^2\boldsymbol{P}_{i-1}\boldsymbol{a}_i\boldsymbol{a}_i^*\boldsymbol{P}_{i-1} \tag{2.39}$$

except that these recursions apply for all i and are initialized by

$$M_{\mathcal{X}_{(-1)}} = 0, \quad \boldsymbol{P}_{-1} = \boldsymbol{R}_h, \quad \text{and} \quad \hat{\underline{\boldsymbol{h}}}_{-1} = \mathbf{0}$$

Now, R is the optimal value for the regularized objective function in (2.33), and $M_{\mathcal{X}_{(i)}}$ is the value of the cost function for the sequence $\boldsymbol{\mathcal{X}}_{(i)}$ up to the time index i. If the value R can be estimated, we can restrict the search of the blind ML solution $\hat{\boldsymbol{\mathcal{X}}}$ to the offsprings of those partial sequences $\boldsymbol{\mathcal{X}}_{(i)}$ which satisfy $M_{\mathcal{X}_{(i)}} < R$.

There are three advantages for this second approach:

1. We don't need to wait for $L+1$ $\mathcal{X}(i)$'s before starting to get a nonzero objective function.

2. We don't need to perform a size $L+1$ matrix inversion as in (2.32); instead a simpler RLS can be performed from the first step.

3. We make use of the channel autocorrelation which will improve the accuracy of the algorithm.

2.3.1 Exact Blind Algorithm

In this section, we describe the algorithm that we use to find the ML solution of the system output observations, the algorithm employs the above set of iterations (2.35)−(2.39) to update the value of the cost function ($M_{\mathcal{X}_{(i)}}$) which we need for the comparison with the estimated value R (we denote it in the blind algorithm below as the search radius r).

The input parameters for this algorithm are:

- The received channel output $\boldsymbol{\mathcal{Y}}$.
- The search radius r.
- The modulation constellation Ω.
- $1\times N$ index vector I.

We denote the kth constellation point in the modulation constellation Ω as $\Omega(k)$.

The following steps explain the process of our algorithm, which we illustrate them also in the next flowchart (Figure (2.1)):

1. Set $i = 1$, $r_i = r$, $I(i) = 1$ and set $\mathcal{X}(i) = \Omega(I(i))$.
2. (Computing the bounds) Compute the metric $M_{\mathcal{X}_{(i)}}$. If $M_{\mathcal{X}_{(i)}} > r$, go to 3; else, go to 4;
3. (Backtracking) Find the largest $1 \leq j \leq i$ such that $I(j) < |\Omega|$. If there exists such j, set $i = j$ and go to 5; else go to 6.
4. If $i = N$, store current $\boldsymbol{\mathcal{X}}_{(N)}$, update $r = M_{\mathcal{X}_{(N)}}$ and go to 3; else set $i = i + 1, I(i) = 1$ and $\mathcal{X}(i) = \Omega(I(i))$, go to 2.
5. Set $I(i) = I(i) + 1$ and $\mathcal{X}(i) = \Omega(I(i))$. Go to 2.
6. If any sequence $\boldsymbol{\mathcal{X}}_{(N)}$ is ever found in Step 4, output the latest stored full-length sequence as ML solution; otherwise, double r and go to 1.

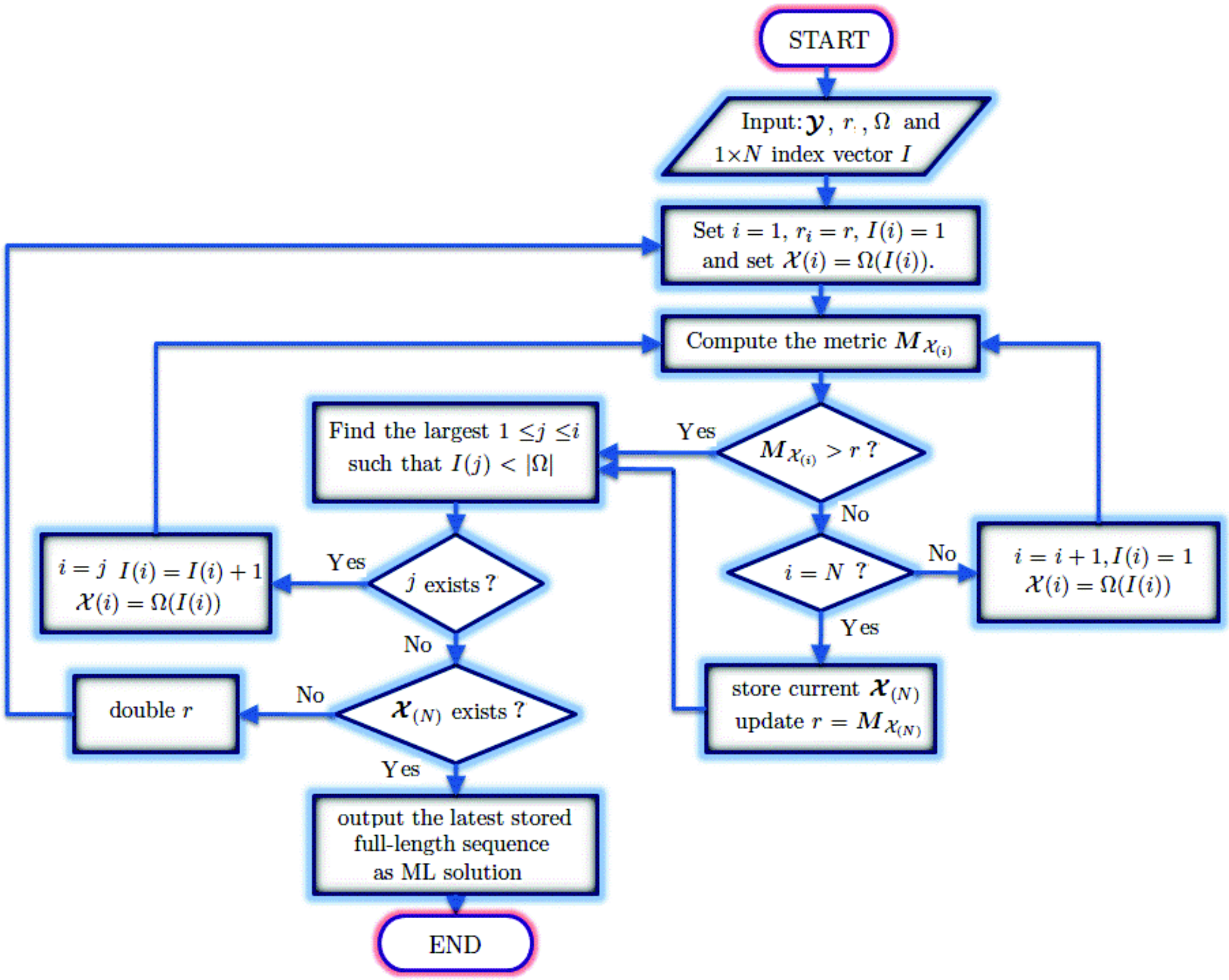

Figure 2.1: Blind Algorithm Flowchart

2.3.2 Choice of the Initial Radius r

The structure of the new blind ML algorithm easily suggests a probabilistic choice of the search radius. We know that $\|\boldsymbol{n}\|^2$ is chisquare distributed with $2N$ degrees of freedom, it is natural to choose the radius r such that $P(\|\boldsymbol{n}\|^2 > r^2) \le 1-\epsilon$. Since the solution R to the optimization problem in (2.33) is sure to be smaller than $\|\boldsymbol{n}\|^2$, we will guarantee finding the blind ML data sequence with probability at least $1-\epsilon$ under this initial radius.

2.4 Blind Equalization in the Constant Modulus Case

As we saw, the backtracking algorithm depends heavily on calculating the cost function. This operation can be made easier in the constant modulus case.

In this case, the values of $\frac{1}{\sigma^2}|\mathcal{X}(i)|^2$ in equations (2.38) and (2.39) become constant for all i, so assume that they are equal to $\frac{1}{\sigma^2}\mathcal{E}_{\mathcal{X}}$, then the values of $\gamma(i)$ and $\boldsymbol{P}_i$ in the same equations will become

$$\gamma(i) = \frac{1}{1 + \frac{1}{\sigma^2}\mathcal{E}_{\mathcal{X}}\boldsymbol{a}_i^*\boldsymbol{P}_{i-1}\boldsymbol{a}_i} \quad (2.40)$$

$$\boldsymbol{P}_i = \boldsymbol{P}_{i-1} - \frac{1}{\sigma^2}\mathcal{E}_{\mathcal{X}}\gamma(i)\boldsymbol{P}_{i-1}\boldsymbol{a}_i\boldsymbol{a}_i^*\boldsymbol{P}_{i-1} \quad (2.41)$$

which are independent of the transmitted signal, and depends only on i, so they are constant for each OFDM symbol and we can calculate them offline. This case will reduce the computational complexity as the $(L+1) \times (L+1)$ matrix $\boldsymbol{P}_i$ will be computed offline and there is no need to update it.

2.5 Drawbacks of the Backtracking Algorithm

Using the above blind algorithm to search for the optimal $\boldsymbol{\mathcal{X}}$ can be computationally very complex due to two main reason:

1. ***Calculating $\boldsymbol{P}_i$:*** the second step of the blind algorithm rely on updating the metric $M_{\mathcal{X}_{(N)}}$, This metric depends heavily on calculating the $L+1 \times L+1$

matrix $\boldsymbol{P}_i$ which adds much complexity to the algorithm.

2. ***Backtracking:*** the main disadvantage of our blind algorithm include in the third step where the algorithm try to improve the detection by searching for best combination of the constellation points that investigate the condition of $M_{\mathcal{X}_{(i)}} > r$.

In the next two sections, we propose approximate methods to avoid these drawbacks, where the both drawbacks can be done jointly or independently.

2.6 Approximate Methods to Reduce the Computational Complexity Involved in Calculating $\boldsymbol{P}_i$

The first drawback makes the blind algorithm more complex due to calculating the matrix $\boldsymbol{P}_i$ at each updating of the metric $M_{\mathcal{X}_{(i)}}$. In the following, we describe two methods to avoid computing this matrix:

2.6.1 Avoiding $\boldsymbol{P}_i$

If we set $\boldsymbol{R}_h$ (the initial value of $\boldsymbol{P}_i$ in the RLS algorithm) equal to the Identity Matrix ($\boldsymbol{I}$), let's see how $\boldsymbol{P}_i$ looks like, note that in equations (2.37)$-$(2.39) $\boldsymbol{P}_i$ always appears multiple by $\boldsymbol{a}_i$, so let's demonstrate how setting $\boldsymbol{P}_{-1} = \boldsymbol{I}$ will reduce our calculations. Start with $i = 0$

$$\gamma(0) = \frac{1}{1 + \frac{1}{\sigma^2}|\mathcal{X}(0)|^2 \boldsymbol{a}_0^* \boldsymbol{P}_{-1} \boldsymbol{a}_0}$$

where $\boldsymbol{a}_i^* \boldsymbol{a}_i = L+1$ and $\boldsymbol{P}_{-1} = \boldsymbol{I}$, then

$$\gamma(0) = \frac{1}{1 + \frac{1}{\sigma^2}|\mathcal{X}(0)|^2(L+1)}$$

and

$$\boldsymbol{P}_0 = \boldsymbol{P}_{-1} - \frac{1}{\sigma^2}\gamma(0)|\mathcal{X}(0)|^2 \boldsymbol{P}_{-1}\boldsymbol{a}_0\boldsymbol{a}_0^*\boldsymbol{P}_{-1}$$

multiply $\boldsymbol{P}_0$ by $\boldsymbol{a}_1$

$$\boldsymbol{P}_0\boldsymbol{a}_1 = \boldsymbol{P}_{-1}\boldsymbol{a}_1 - \frac{1}{\sigma^2}\gamma(0)|\mathcal{X}(0)|^2 \boldsymbol{a}_0\boldsymbol{a}_0^*\boldsymbol{a}_1$$

Since $\boldsymbol{a}_i$ is truncated length$-(L+1)$ FFT vector, we can assume that the value of $\boldsymbol{a}_i^*\boldsymbol{a}_{i-1} \approx \boldsymbol{a}_{i-1}^*\boldsymbol{a}_i \approx 0$,[3] thus

$$\boldsymbol{P}_0\boldsymbol{a}_1 = \boldsymbol{I}\boldsymbol{a}_1 - 0 = \boldsymbol{a}_1 \tag{2.42}$$

Also, multiply $\boldsymbol{P}_0$ by $\boldsymbol{a}_2$ to get

$$\begin{aligned} \boldsymbol{P}_0\boldsymbol{a}_2 &= \boldsymbol{P}_{-1}\boldsymbol{a}_2 - \frac{1}{\sigma^2}\gamma(0)|\mathcal{X}(0)|^2 \boldsymbol{a}_0\boldsymbol{a}_0^*\boldsymbol{a}_2 && (2.43) \\ &= \boldsymbol{I}\boldsymbol{a}_2 - 0 = \boldsymbol{a}_2 && (2.44) \end{aligned}$$

For $i = 1$

$$\gamma(1) = \frac{1}{1 + \frac{1}{\sigma^2}|\mathcal{X}(1)|^2 \boldsymbol{a}_1^*\boldsymbol{P}_0\boldsymbol{a}_1}$$

[3]This becomes especially true for large L

from the above equation (2.42), $\boldsymbol{P}_0\boldsymbol{a}_1 = \boldsymbol{a}_1$, thus

$$\gamma(1) = \frac{1}{1 + \frac{1}{\sigma^2}|\mathcal{X}(1)|^2(L+1)}$$

Since $\boldsymbol{P}_0\boldsymbol{a}_1 = \boldsymbol{a}_1$ and $\boldsymbol{P}_0\boldsymbol{a}_2 = \boldsymbol{a}_2$ (from equations (2.42) and (2.44), respectively), the value of $\boldsymbol{P}_1\boldsymbol{a}_2$ is given by

$$\boldsymbol{P}_1\boldsymbol{a}_2 = \boldsymbol{P}_0\boldsymbol{a}_2 - \frac{1}{\sigma^2}\gamma(1)|\mathcal{X}(1)|^2\boldsymbol{P}_0\boldsymbol{a}_1\boldsymbol{a}_1^*\boldsymbol{P}_0\boldsymbol{a}_2 \tag{2.45}$$

$$= \boldsymbol{a}_2 - \frac{1}{\sigma^2}\gamma(1)|\mathcal{X}(1)|^2\boldsymbol{a}_1\boldsymbol{a}_1^*\boldsymbol{a}_2 \tag{2.46}$$

$$= \boldsymbol{a}_2 \tag{2.47}$$

Now, from the above equations (2.42)-(2.47) we can assume that $\boldsymbol{P}_i\boldsymbol{a}_{i+1} = \boldsymbol{a}_{i+1}$, and $\boldsymbol{P}_i\boldsymbol{a}_{i+2} = \boldsymbol{a}_{i+2}$, so let's prove also that $\boldsymbol{P}_{i+1}\boldsymbol{a}_{i+2} = \boldsymbol{a}_{i+2}$

$$\boldsymbol{P}_{i+1}\boldsymbol{a}_{i+2} = \boldsymbol{P}_i\boldsymbol{a}_{i+2} - \frac{1}{\sigma^2}\gamma(i+1)|\mathcal{X}(i+1)|^2\boldsymbol{P}_i\boldsymbol{a}_{i+1}\boldsymbol{a}_{i+1}^*\boldsymbol{P}_i\boldsymbol{a}_{i+2} \tag{2.48}$$

$$= \boldsymbol{a}_{i+2} - \frac{1}{\sigma^2}\gamma(i+1)|\mathcal{X}(i+1)|^2\boldsymbol{a}_{i+1}\boldsymbol{a}_{i+1}^*\boldsymbol{a}_{i+2} \tag{2.49}$$

$$= \boldsymbol{a}_{i+2} \tag{2.50}$$

As a result, the values of $\gamma(i)$ and $\boldsymbol{P}_i\boldsymbol{a}_{i+1}$ are given by

$$\gamma(i) = \frac{1}{1 + \frac{1}{\sigma^2}|\mathcal{X}(i)|^2(L+1)}, \quad \text{for} \quad i = 0, 1, \ldots, N-1 \tag{2.51}$$

$$\boldsymbol{P}_i\boldsymbol{a}_{i+1} = \boldsymbol{a}_{i+1} \tag{2.52}$$

Use this result in our blind RLS algorithm in (2.35)-(2.39) and replace $\boldsymbol{g}_i$ and $\hat{\underline{\boldsymbol{h}}}_i$ by the following equations.

$$\boldsymbol{g}_i = \frac{1}{\sigma}\gamma(i)\mathcal{X}^*(i)\boldsymbol{a}_i \tag{2.53}$$

$$\boxed{\hat{\underline{\boldsymbol{h}}}_i = \hat{\underline{\boldsymbol{h}}}_{i-1} + \tfrac{1}{\sigma^2}\gamma(i)[\mathcal{X}^*(i)\mathcal{Y}(i)\boldsymbol{a}_i - |\mathcal{X}(i)|^2\boldsymbol{a}_i\boldsymbol{a}_i^*\hat{\underline{\boldsymbol{h}}}_{i-1}]} \tag{2.54}$$

Observe that our blind algorithm remain same except that we don't need to calculate the value of $\boldsymbol{P}_i$ in equation (2.39), which drastically reduces the computational complexity. In the next section, we shall compare the computational complexity for this method and the blind RLS algorithm.

Constant Modulus Case

Let's apply this method to the constant modulus case and see how the calculations become simpler. We know that the values of $\frac{1}{\sigma^2}|\mathcal{X}(i)|^2$ become constant for all i and equal to $\frac{1}{\sigma^2}\mathcal{E}_\mathcal{X}$ in the constant modulus case. So the above values of $\gamma(i)$ and $\hat{\underline{\boldsymbol{h}}}_i$ in (2.51) and (2.54), respectively, become

$$\gamma(i) = \frac{1}{1 + \frac{1}{\sigma^2}\mathcal{E}_\mathcal{X}(L+1)} \tag{2.55}$$

$$\hat{\underline{\boldsymbol{h}}}_i = \hat{\underline{\boldsymbol{h}}}_{i-1} + \frac{1}{1 + \frac{1}{\sigma^2}\mathcal{E}_\mathcal{X}(L+1)}(\frac{1}{\sigma}\mathcal{X}^*(i))(\frac{1}{\sigma}\mathcal{Y}(i))\boldsymbol{a}_i - \frac{1}{\sigma^2}\mathcal{E}_\mathcal{X}\boldsymbol{a}_i\boldsymbol{a}_i^*\hat{\underline{\boldsymbol{h}}}_{i-1}$$

take $\frac{1}{\sigma^2}$ as a common factor

$$\boxed{\hat{\underline{\boldsymbol{h}}}_i = \hat{\underline{\boldsymbol{h}}}_{i-1} + \tfrac{1}{\sigma^2 + \mathcal{E}_\mathcal{X}(L+1)}\mathcal{X}^*(i)\mathcal{Y}(i)\boldsymbol{a}_i - \mathcal{E}_\mathcal{X}\boldsymbol{a}_i\boldsymbol{a}_i^*\hat{\underline{\boldsymbol{h}}}_{i-1}} \tag{2.56}$$

In addition to the above result of avoiding $\boldsymbol{P}_i$, we also don't need to calculate $\gamma(i)$, this leads to more reduction in the complexity.

2.6.2 Avoiding $\boldsymbol{P}_i$ with Ordering $\boldsymbol{A}_i^*$

In the previous subsection we have presented a method to reduce the computational complexity assuming that $\boldsymbol{R}_h = \boldsymbol{I}$ and $\boldsymbol{a}_i^* \boldsymbol{a}_{i-1} \approx \boldsymbol{a}_{i-1}^* \boldsymbol{a}_i \approx 0$. In this subsection, we suggest a method to make $\boldsymbol{a}_i^* \boldsymbol{a}_{i-1}$ and $\boldsymbol{a}_{i-1}^* \boldsymbol{a}_i$ equal to zero, which will improve our previous method.

We know that $\boldsymbol{a}_i^*$ is a truncated length$-(L+1)$ FFT vector, and multiplying $\boldsymbol{a}_i^*$ by $\boldsymbol{a}_{i-1}$ is not exactly equal to zero. However, we can order these vectors to become a full FFT vectors such that the values of $\boldsymbol{a}_i^* \boldsymbol{a}_{i-1}$ and $\boldsymbol{a}_{i-1}^* \boldsymbol{a}_i$ become zero. Here, $\boldsymbol{a}_i^*$ is the $i-$th row of the truncated $(N \times (L+1))$ FFT matrix $\boldsymbol{A}^*$

$$\boldsymbol{A}^* = \begin{bmatrix} e^{-j\frac{2\pi}{N}(0)(0)} & e^{-j\frac{2\pi}{N}(0)(1)} & \cdots & e^{-j\frac{2\pi}{N}(0)(L)} \\ e^{-j\frac{2\pi}{N}(1)(0)} & e^{-j\frac{2\pi}{N}(1)(1)} & \cdots & e^{-j\frac{2\pi}{N}(1)(L)} \\ \vdots & \vdots & \vdots & \vdots \\ e^{-j\frac{2\pi}{N}(N-1)(0)} & e^{-j\frac{2\pi}{N}(N-1)(1)} & \cdots & e^{-j\frac{2\pi}{N}(N-1)(L)} \end{bmatrix}_{N\times(L+1)} = \begin{bmatrix} \boldsymbol{a}_0^* \\ \boldsymbol{a}_1^* \\ \vdots \\ \boldsymbol{a}_{N-1}^* \end{bmatrix}$$

where

$$\boldsymbol{a}_n^* = \begin{bmatrix} e^{-j\frac{2\pi}{N}(n)(0)} & e^{-j\frac{2\pi}{N}(n)(1)} & \cdots & e^{-j\frac{2\pi}{N}(n)(L)} \end{bmatrix} \quad \text{for } \ n = 0, 1, ..., N-1$$

In OFDM systems, the cyclic prefix is usually chosen to be $\frac{N}{4}$, $\frac{N}{8}$, $\frac{N}{16}$, etc. So, let's assume that the channel length is equal to the cyclic prefix and take the case of

$L+1=\frac{N}{4}$, in this case $\boldsymbol{a}_n^*$ given by

$$\boldsymbol{a}_n^* = \begin{bmatrix} e^{-j\frac{2\pi}{N}(n)(0)} & e^{-j\frac{2\pi}{N}(n)(1)} & \dots & e^{-j\frac{2\pi}{N}(n)(\frac{N}{4}-1)} \end{bmatrix}$$

Then, let $n=4n'$, where $n'=0,1,...,(\frac{N}{4}-1)$, thus

$$\begin{aligned} \boldsymbol{a}_{4n'}^* &= \begin{bmatrix} e^{-j\frac{2\pi}{N}(4n')(0)} & e^{-j\frac{2\pi}{N}(4n')(1)} & \dots & e^{-j\frac{2\pi}{N}(4n')(\frac{N}{4}-1)} \end{bmatrix} \\ &= \begin{bmatrix} e^{-j\frac{2\pi}{N/4}(n')(0)} & e^{-j\frac{2\pi}{N/4}(n')(1)} & \dots & e^{-j\frac{2\pi}{N/4}(n')(\frac{N}{4}-1)} \end{bmatrix} \end{aligned}$$

and define $\boldsymbol{A}_0^*$ as

$$\boldsymbol{A}_0^* = \begin{bmatrix} \boldsymbol{a}_{4\times 0}^* \\ \boldsymbol{a}_{4\times 1}^* \\ \vdots \\ \boldsymbol{a}_{4\times(\frac{N}{4}-1)}^* \end{bmatrix} = \begin{bmatrix} \boldsymbol{a}_0^* \\ \boldsymbol{a}_4^* \\ \vdots \\ \boldsymbol{a}_{N-4}^* \end{bmatrix} = \begin{bmatrix} e^{-j\frac{2\pi}{N/4}(0)(0)} & e^{-j\frac{2\pi}{N/4}(0)(1)} & \dots & e^{-j\frac{2\pi}{N/4}(0)(\frac{N}{4}-1)} \\ e^{-j\frac{2\pi}{N/4}(1)(0)} & e^{-j\frac{2\pi}{N/4}(1)(1)} & \dots & e^{-j\frac{2\pi}{N/4}(1)(\frac{N}{4}-1)} \\ \vdots & \vdots & \vdots & \vdots \\ e^{-j\frac{2\pi}{N/4}(\frac{N}{4}-1)(0)} & e^{-j\frac{2\pi}{N/4}(\frac{N}{4}-1)(1)} & \dots & e^{-j\frac{2\pi}{N/4}(\frac{N}{4}-1)(\frac{N}{4}-1)} \end{bmatrix}_{\frac{N}{4}\times\frac{N}{4}}$$

where $\boldsymbol{A}_0^*$ has $\frac{N}{4}$ vectors from the matrix $\boldsymbol{A}^*$, this matrix is full $\frac{N}{4}\times\frac{N}{4}$ FFT matrix, i.e. the multiplication of any row with the conjugate transpose of any other one will give zero. We can write $\boldsymbol{A}_0^*$ in general form as $\boldsymbol{A}_l^*$ for $l = 0,\ 1,\ ...,\ (\frac{N}{4} - 1)$ as

$$\boldsymbol{A}_l^* = \begin{bmatrix} \boldsymbol{a}^*_{4\times 0+l} \\ \boldsymbol{a}^*_{4\times 1+l} \\ \boldsymbol{a}^*_{4\times 2+l} \\ \vdots \\ \boldsymbol{a}^*_{4\times(\frac{N}{4}-1)+l} \end{bmatrix} = \begin{bmatrix} \boldsymbol{a}^*_{0+l} \\ \boldsymbol{a}^*_{4+l} \\ \boldsymbol{a}^*_{8+l} \\ \vdots \\ \boldsymbol{a}^*_{(N-4)+l} \end{bmatrix}$$

where

$$\boldsymbol{a}^*_{n+l} = \begin{bmatrix} e^{-j\frac{2\pi}{N}(n+l)(0)} & e^{-j\frac{2\pi}{N}(n+l)(1)} & \cdots & e^{-j\frac{2\pi}{N}(n+l)(\frac{N}{4}-1)} \end{bmatrix}$$

So, to get the same result for the whole matrix $\boldsymbol{A}^*$ we have to take out these full matrices from $\boldsymbol{A}^*$ and arrange them again as follows:

$$\boldsymbol{A}^* = \begin{bmatrix} \boldsymbol{A}_0^* \\ \boldsymbol{A}_1^* \\ \vdots \\ \boldsymbol{A}^*_{\frac{N}{4}-1} \end{bmatrix}$$

As a result, we can ensure here that the value of $(\boldsymbol{a}_i^*\boldsymbol{a}_{i-1})$ and $(\boldsymbol{a}_{i-1}^*\boldsymbol{a}_i)$ equal to zero.[4] Since, we just assume that the weighting matrix $\boldsymbol{R}_h$ is equal to Identity matrix ($\boldsymbol{I}$) without any other assumption, this method give better performance than the previous one as we will see in the simulation results.

[4]This becomes true only when the channel length $(L+1) = \frac{N}{4},\ \frac{N}{8},\ \frac{N}{16}$, etc.

2.7 Minimum Cost Method

In addition to calculating the $(L+1)\times(L+1)$ matrix $\boldsymbol{P}_i$ in the backtracking algorithm, there is a backtracking operation steps which increase its complexity. In the following, we describe a method to avoid these steps.

Our objective in data detection is to minimize the cost function. In this method, we depend on finding the constellation points that minimize the cost function at each carrier (according to the following equation (2.57)) and take them as a solution without backtracking.

From (2.35), and for the j-th constellation point $(\Omega(j))$, we can define $M^j_{\mathcal{X}_{(i)}}$ as the cost function up to the time index i, say

$$\boxed{M^j_{\mathcal{X}_{(i)}} = M_{\mathcal{X}_{(i-1)}} + \tfrac{1}{\sigma^2}\gamma(i)|\mathcal{Y}(i) - \Omega(j)\boldsymbol{a}_i^*\underline{\hat{\boldsymbol{h}}}_{i-1}|^2} \tag{2.57}$$

After we compute all the j values of the cost function, we find the minimum one and its index (l), then store the l-th constellation point in the i-th solution $\hat{\mathcal{X}}(i)$. The same procedure is followed for the next carrier up to the one at time N. The following flowchart (Figure (2.2))explains the processes of our approach. We denote the number of the constellation points as m.

In this method, there is no need to do backtracking, which gives us a very low complexity compared with backtracking method (Figure (2.1)) with some sacrifice in the BER performance as we will show in the simulation results.

In addition, this method can be used as a pilot based channel estimation method

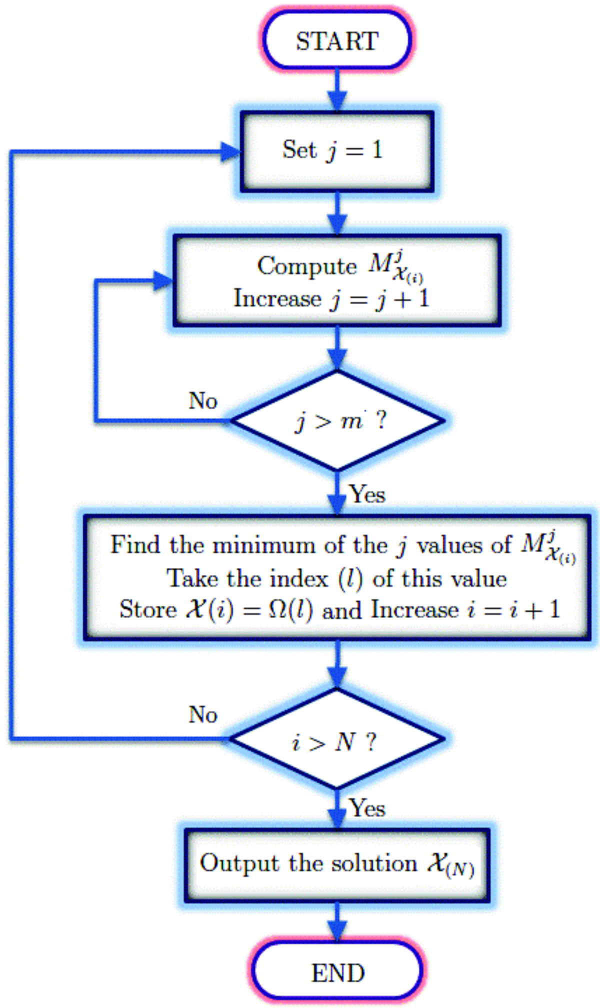

Figure 2.2: Flowchart of the Minimum Cost Method

when we use some training symbols at the receiver.

2.8 Computational Complexity Comparison

In this section, we provide a comparison of our blind algorithm and the three approximate methods. We start by giving the estimated number of real multiplications and real additions that are required in the evaluation of specific terms of the RLS

Table 2.1: Estimated computational cost per iteration of the RLS algorithm

Term	$\times$	$+$	$\div$
$\mathcal{X}(i)\boldsymbol{a}_i^*\hat{\underline{\boldsymbol{h}}}_{i-1}$	$2k$	$k-1$	
$\lvert\mathcal{Y}(i)-\mathcal{X}(i)\boldsymbol{a}_i^*\hat{\underline{\boldsymbol{h}}}_{i-1}\rvert^2$	1	1	
$\frac{1}{\sigma^2}\gamma(i)$	1		1
$M_{\mathcal{X}_{(i)}}$	1	1	
$\hat{\underline{\boldsymbol{h}}}_i$	$k+1$	k	1
$\boldsymbol{P}_{i-1}\boldsymbol{a}_i$	k^2	$k(k-1)$	
$\boldsymbol{g}_i$	$k+2$		
$\boldsymbol{a}_i^*\boldsymbol{P}_{i-1}\boldsymbol{a}_i$	k	$k-1$	
$\gamma(i)$	3	1	1
$\boldsymbol{a}_i^*\boldsymbol{P}_{i-1}$	k^2	$k(k-1)$	
$\boldsymbol{P}_i$	k^2+1	k^2	
Total per iteration	$3k^2+5k+9$	$2k^2+k+1$	3

Table 2.2: Estimated computational cost per iteration of the RLS algorithm without calculating $\boldsymbol{P}_i$

Term	$\times$	$+$	$\div$
$\mathcal{X}(i)\boldsymbol{a}_i^*\hat{\underline{\boldsymbol{h}}}_{i-1}$	$2k$	$k-1$	
$\lvert\mathcal{Y}(i)-\mathcal{X}(i)\boldsymbol{a}_i^*\hat{\underline{\boldsymbol{h}}}_{i-1}\rvert^2$	1	1	
$\frac{1}{\sigma^2}\gamma(i)$	1		1
$M_{\mathcal{X}_{(i)}}$	1	1	
$\hat{\underline{\boldsymbol{h}}}_i$	$k+1$	k	1
$\gamma(i)$	3	1	1
Total per iteration	$4k+9$	$2k+2$	3

algorithm and the two methods of avoiding $\boldsymbol{P}_i$ for real data case,[5] in Tables 2.1 and 2.2, respectively. Here, k is the length of the channel, N is the length of the data sequence and m is the size of the symbol alphabet.

Table 2.3 lists the estimated computational cost per iteration for the blind RLS algorithm with and without calculating $\boldsymbol{P}_i$ and the minimum cost methods, assuming real data. The costs are in terms of the number of multiplications and additions that are needed for each iteration. We assume that the computational cost of the blind

[5]The two methods of avoiding $\boldsymbol{P}_i$ give the same computational cost, so we compare the RLS algorithm with one of them.

Table 2.3: Computational cost comparison for OFDM blind algorithms

Algorithm	$\times$	$+$
Blind RLS algorithm	$(3k^2+5k+9)f(N)$	$(2k^2+k+1)f(N)$
Blind RLS alg. without calculating $\boldsymbol{P}_i$	$(4k+9)f(N)$	$(2k+2)f(N)$
Minimum cost method	$(3k^2+5k+9)m$	$(2k^2+k+1)m$

algorithm described in Subsection 2.3.1 as a function of N per iteration ($f(N)$), thus the computational complexity of the *blind RLS algorithm* with and without calculating $\boldsymbol{P}_i$ will be multiplied by this function because the blind algorithm needs to compute the cost function $M_{x^*_{(i)}}$ using the RLS algorithm for each backtracking operation.

The minimum cost method computes the cost function ($M_{x^*_{(i)}}$) m times per iteration using the RLS algorithm. So, its computational cost will be m times the computational cost of the RLS algorithm.

It is seen from Table 2.3 that the blind RLS algorithm requires ($O(k^2)f(N)$) operations per iteration, while when we use it without calculating $\boldsymbol{P}_i$ the computational cost reduced to ($O(k)f(N)$) operations per iteration.

2.9 Simulation Results

This section is divided into three parts. In the first part, simulation results of the blind equalization are discussed. In the second part, we provide results for the three approximate methods while in the third part, we show how using some pilots could enhance the BER performance.

2.9.1 Blind Equalization

In this section, we give simulation results for the performance of the new blind algorithm. We investigate its performance in OFDM system employing BPSK, 4QAM and 16QAM modulation data where we assume $N = 16$ carriers and cyclic prefix of length $L = \frac{N}{4} - 1$. In the simulation, the channel IR consists of $L + 1$ iid Rayleigh fading taps which remains constant over one OFDM symbol. We compare the BER performance of four methods: (i) Perfectly known channel, (ii) Channel estimated using $L + 1$ pilots and (iii) The new Blind Algorithm.

BER vs SNR Comparison for BPSK Modulated Data

In Figure 2.3, we compare the three mentioned approaches and a semiblind least squares estimator using $L + 1$ pilots and frequency correlation, for BPSK modulated data over a Rayleigh fading channel. As expected, the best performance is achieved by the perfectly known channel, followed by that obtained by the semiblind least squares estimator using $L + 1$ pilots and frequency correlation. The simulation also shows favorable BER performance of the blind equalization method comparing with the method that using $L + 1$ pilots in channel estimation.

BER vs SNR Comparison for QAM Modulated Data

The same conclusion can be made for 4QAM and 16QAM (non-constant modulus) modulation (see Figures 2.4 and 2.5), where the blind algorithm outperforms the pilot based estimation method at high SNR.

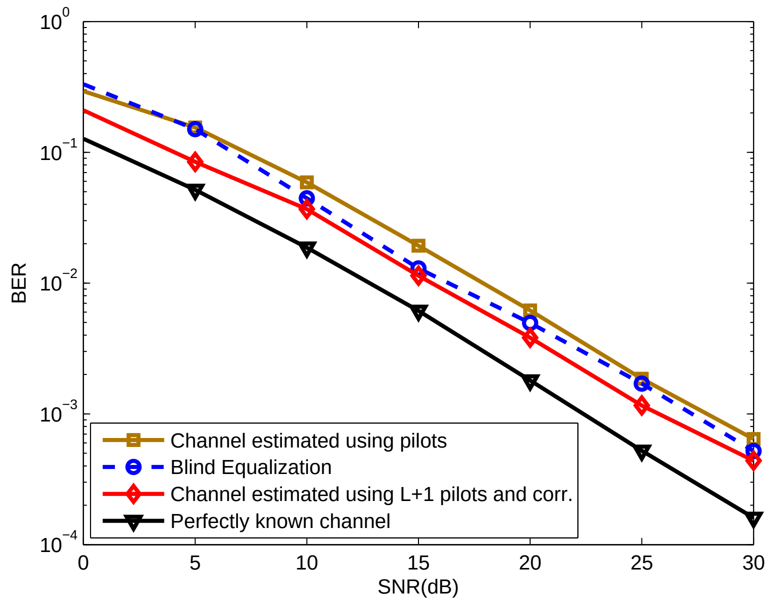

Figure 2.3: BER vs SNR for BPSK-OFDM over a Rayleigh channel

BER Performance for 4QAM Modulated Data without using $\boldsymbol{R}_h$

In the previous subsections, we assumed that the receiver has some information about the channel which is the autocorrelation matrix ($\boldsymbol{R}_h$). Here, we consider a more realistic case when the receiver doesn't have any information about the channel. Figure 2.6 shows the comparison between these two cases. As we see the second case performs very close to the first one which means that our algorithm is totaly blind.

2.9.2 Approximate Methods

In this section, we give simulation results for the performance of the three approximate methods proposed in Sections 2.6 and 2.7 for BPSK and 4QAM input data. We consider the same OFDM system used in the previous subsection.

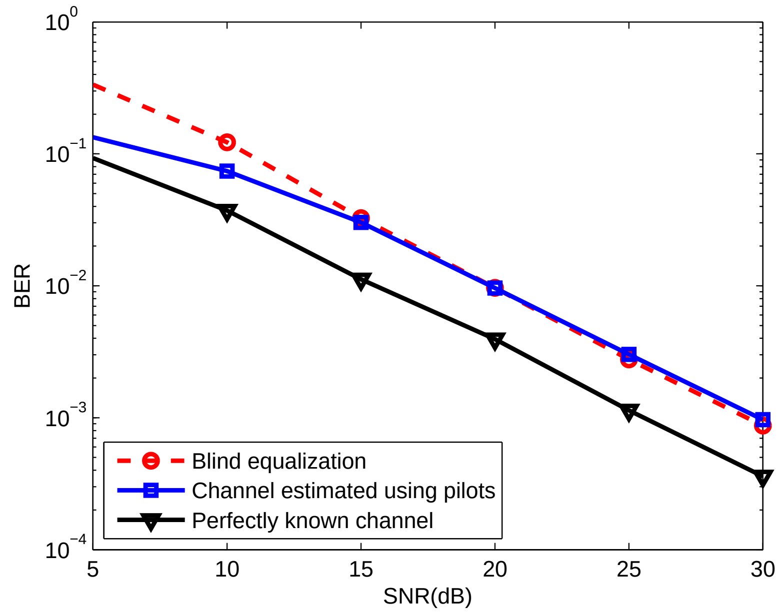

Figure 2.4: BER vs SNR for 4QAM-OFDM over a Rayleigh channel

Comparison of low complexity algorithms for BPSK modulated data

Figure 2.7 show the BER performance comparison between the backtracking method and the three low computational complexity methods i.e. Avoiding $\boldsymbol{P}_i$, Avoiding $\boldsymbol{P}_i$ with ordering $\boldsymbol{A}^*$ and the minimum cost method, for BPSK input data. As we see the second method gives better performance than the others and it is very close to the backtracking method.

Comparison of low complexity algorithms for 4QAM modulated data

Here, for 4QAM input data (see Figure 2.8), the same conclusion of the BPSK case can be made, namely, the second method performs quite close to the blind equalization.

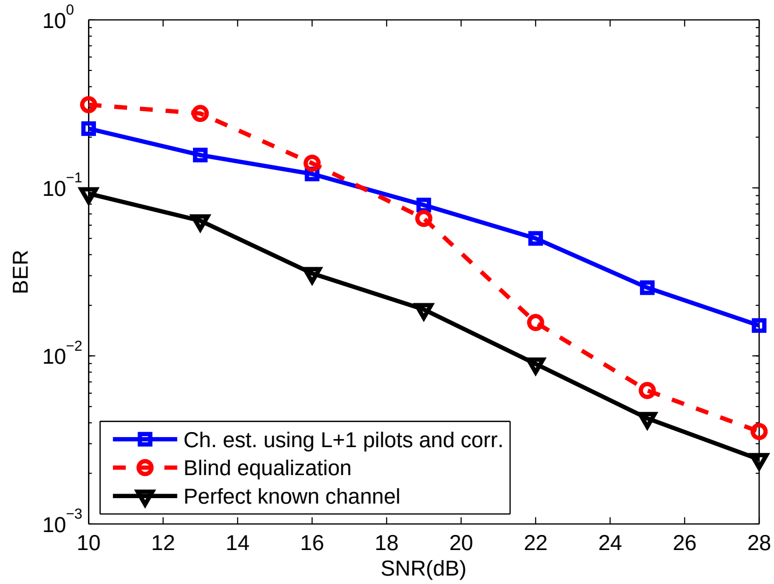

Figure 2.5: BER vs SNR for 16QAM-OFDM over a Rayleigh channel

Comparison of minimum cost method for BPSK modulated data

The minimum cost method described in Section 2.7 was implemented using some pilots. We give here a simulation result for more realistic OFDM system with $N = 64$ carriers and 16 Rayleigh fading channel taps. Figure 2.9 shows the performance of the minimum cost method for the BPSK input data using 12 pilots comparing with perfectly known channel and pilot based estimation using 12 pilots. It can be seen that the pilots based method reaches an error floor at high SNR while the minimum cost method performs better.

Comparison of minimum cost method for 16QAM modulated data

Figure 2.10 shows the performance of the minimum cost method for the 16QAM input data with $N = 16$ carriers and 4 Rayleigh fading channel taps using L+1 pilots

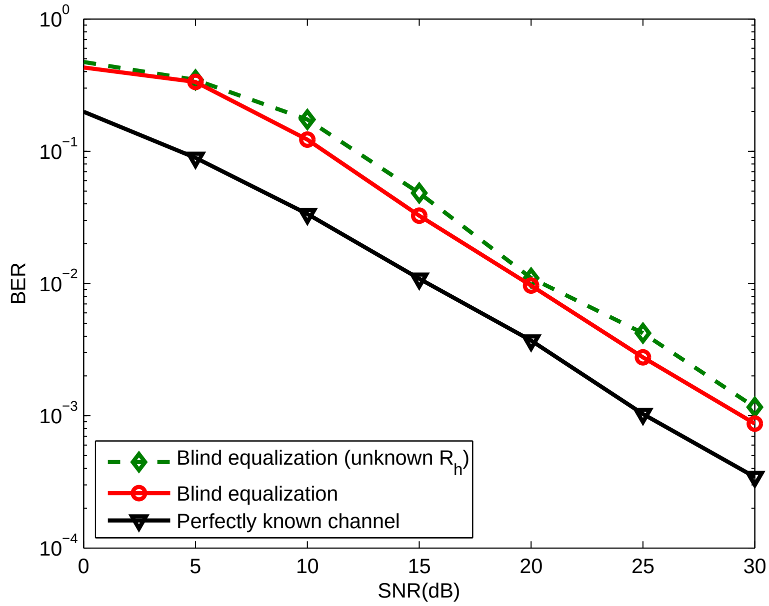

Figure 2.6: BER vs SNR for 4QAM-OFDM without using channel information

comparing with perfectly known channel and pilot based estimation using L+1 pilots. It can be seen that the minimum cost method improves upon the pilot based channel estimation method by approximately 5 dB. The same conclusion can be made in Figure 2.11 with 2 dB improvement in the performance at high SNR for 16QAM modulated data with $N = 64$ carriers and 8 Rayleigh fading channel taps.

2.9.3 Enhanced Equalization Using Pilots

In the above two subsections, we embed one known data symbol in the OFDM symbol to resolve the phase ambiguity and to initialize the RLS algorithm used in the blind equalization. Here, we use some pilots to enhance the equalization. We consider an OFDM system with $N = 16$ and $L = 3$.

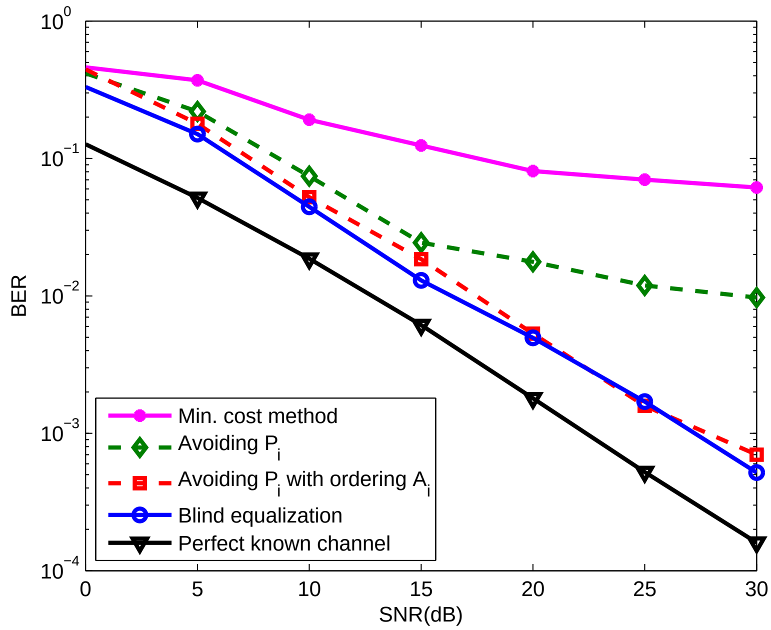

Figure 2.7: Comparison of low complexity algorithms for BPSK-OFDM

BER vs SNR Comparison for BPSK Modulated Data

Figure 2.12 shows the performance of the receiver with enhanced equalization using some pilots for BPSK modulated data over a Rayleigh channel. It can be seen that using of 2 pilots give better performance than the method of channel estimation using $L+1$ pilots and correlation and works very close to the perfectly known channel case at high SNR.

BER vs SNR Comparison for 4QAM Modulated Data

The performance of the receiver with enhanced equalization using pilots for 4QAM modulated data is shown in Figure 2.13. Similar to the BPSK modulated data case, the receiver with 3 pilots shows better BER performance than the method of channel estimation using pilots.

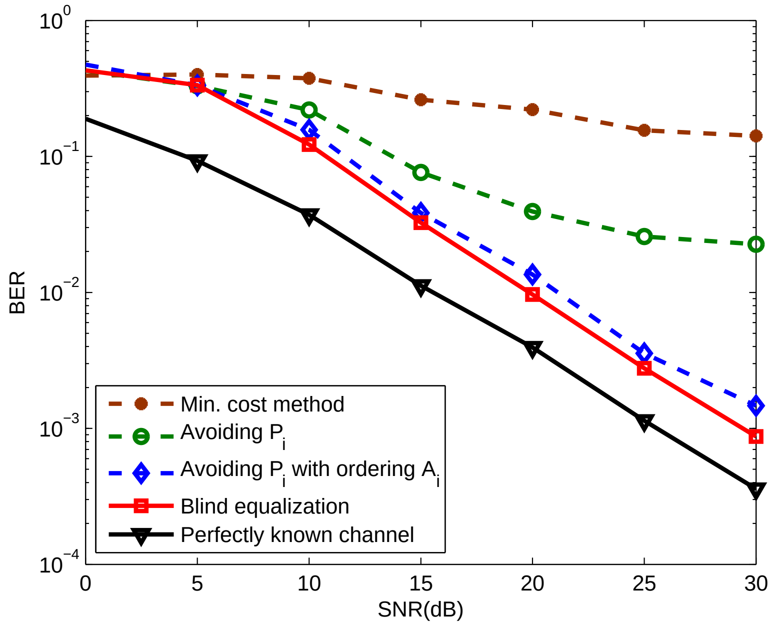

Figure 2.8: Comparison of low complexity algorithms for 4QAM-OFDM

2.10 Conclusion

In this chapter, we demonstrated how to perform blind equalization in OFDM transmission. We propose a low-complexity blind algorithm which achieves the exact ML data detection for OFDM wireless systems employing data with general constellations. The algorithm is able to recover the data from the output observations only. Simulation results showed the favorable performance of the algorithm for many constellations including the constant modulus (BPSK and 4QAM) and non-constant modulus (16QAM) constellations. We stress that the estimation is done on a (OFDM) symbol by symbol basis allowing the algorithm to deal with fast block fading channels.

We have also proposed three approximate methods (avoiding $\boldsymbol{P}_i$, avoiding $\boldsymbol{P}_i$ with ordering $\boldsymbol{A}_i$ and minimum cost methods) to reduce the computational complexity en-

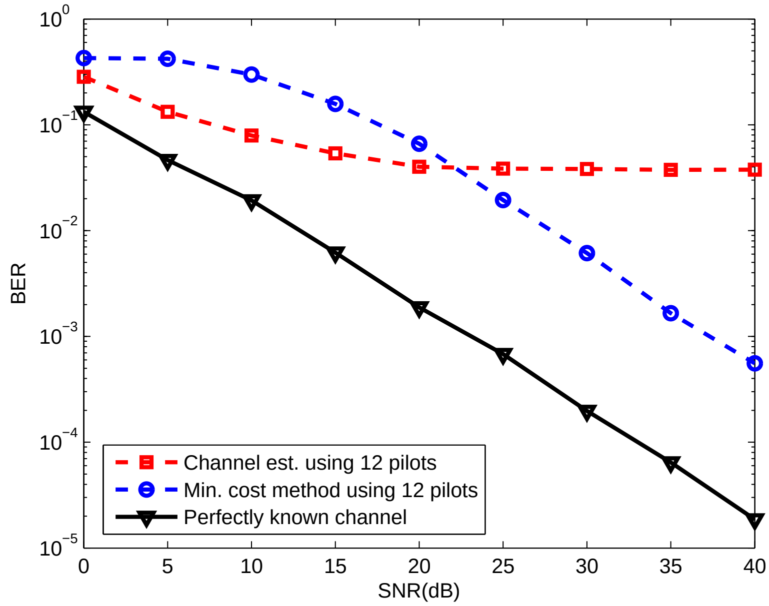

Figure 2.9: Comparison of minimum cost method for BPSK-OFDM with $N = 64$ and $L = 15$ over a Rayleigh channel

tailed in the algorithm developed in the chapter. It was found that using the second method performed better than all other methods proposed. We can consider the minimum cost method as a pilot based estimation technique which performs better than the pilot based estimation method. As is evident from the simulation results, some of these approximate methods perform quite close to the exact blind ML detection algorithm.

As all standard-based OFDM systems involve some form of training, we have also studied the behavior of the blind receiver in the presence of pilots.

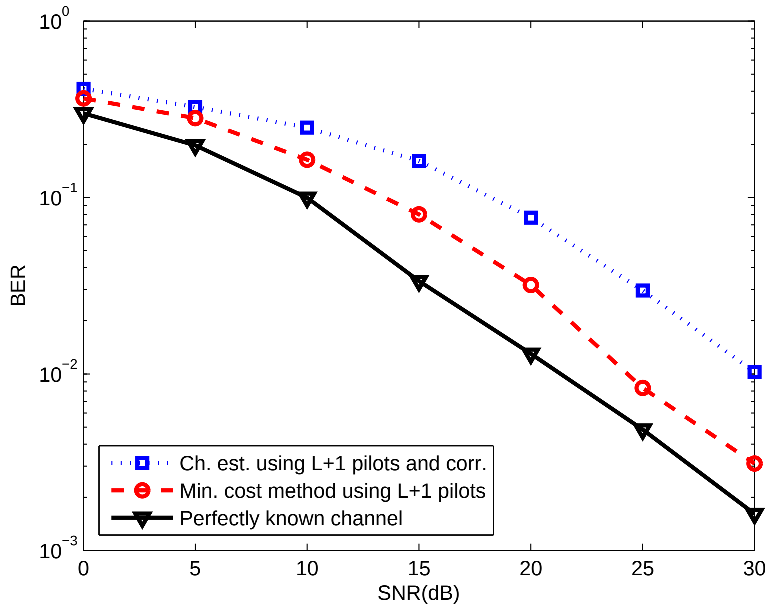

Figure 2.10: Comparison of minimum cost method for 16QAM-OFDM with $N = 16$ and $L = 3$ over a Rayleigh channel

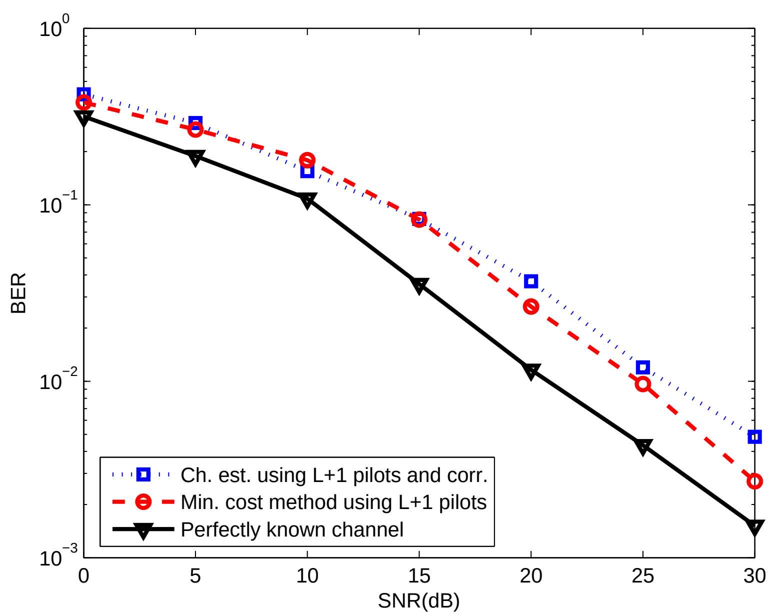

Figure 2.11: Comparison of minimum cost method for 16QAM-OFDM with $N = 64$ and $L = 7$ over a Rayleigh channel

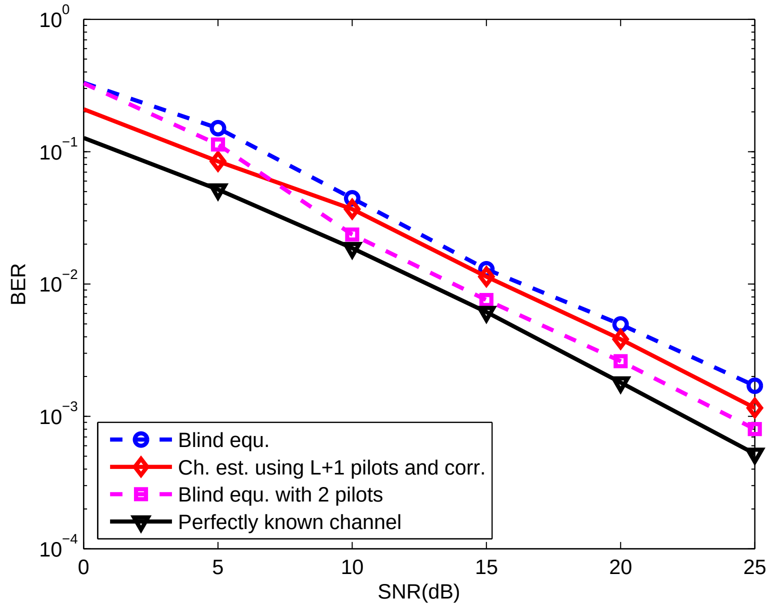

Figure 2.12: BER vs SNR for BPSK-OFDM over a Rayleigh channel

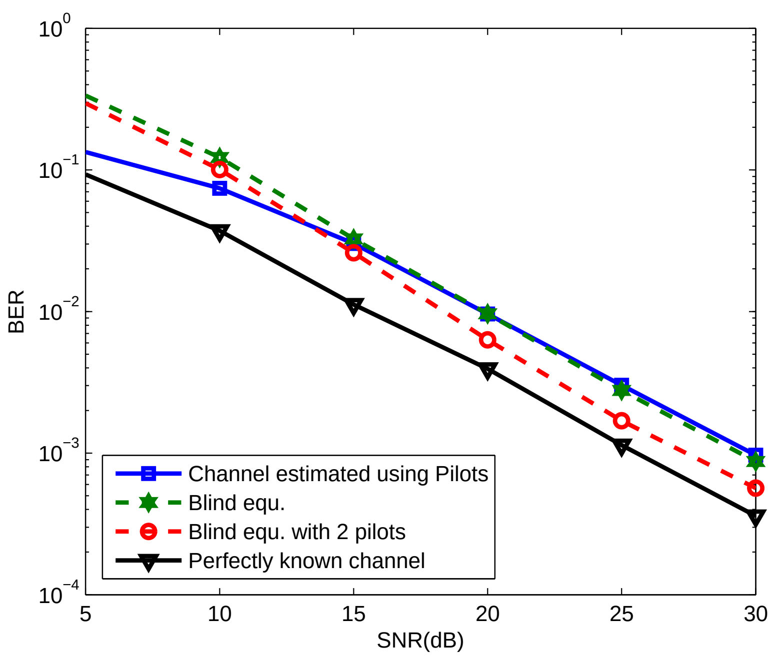

Figure 2.13: BER vs SNR for 4QAM-OFDM over a Rayleigh channel

CHAPTER 3

BLIND EQUALIZATION FOR LINEAR CONVOLUTION SISO SYSTEMS

3.1 Introduction

The demand for high data rate reliable communications poses great challenges to the next generation wireless systems in highly dynamic mobile environments. In this chapter, we investigate the joint Maximum-Likelihood (ML) channel estimation and signal detection problem for Single-Input Single-Output (SISO) wireless systems with general modulation constellations and propose an efficient algorithm for finding the exact joint ML solution. Unlike other known methods, the new algorithm can even efficiently find the joint ML solution under high spectral efficiency non constant modulus modulation constellations. In particular, the new algorithm does not need such preprocessing steps as Cholesky or QR decomposition in the traditional sphere decoders for joint ML channel estimation and data detection.

3.1.1 The Approach and Organization of the Chapter

This chapter considers blind receiver design for SISO transmission over block fading channels. The receiver employs the maximum likelihood (ML) algorithm for joint channel and data recovery. It makes collective use of the data and channel constraints that characterize the communication problem. The data constraints include the finite alphabet constraint. The channel constraints include the finite delay spread and frequency and time correlation.

We perform data identification and equalization from output observations only, without the need for a training sequence or a priori channel information. The advantage of our approach is three fold:

1. The method provides a *blind detection* of the data from one output data packet without the need for training.

2. The algorithm works on linear convolution SISO systems employing data with *general constellations*.

3. Data equalization is done *without* any restriction on the channel.

This chapter is organized as follows. We give an overview of the system in Section 3.2. Section 3.3 then presents our approach, while Section 3.4 proposes an algorithm to reduce the complexity involved in the proposed blind algorithm, while another low complexity equalization method is proposed in section 3.5. We compare the computational complexities of the various algorithms in Section 3.6, and Section 3.7 shows our simulations. We conclude the chapter in Section 3.8.

3.2 System Overview

Let us consider a SISO system with N be the length of a data packet during which the channel remains static. Then the channel output is written as

$$\boldsymbol{y} = \boldsymbol{h} * \boldsymbol{x}^* + \boldsymbol{n} \tag{3.1}$$

where $\boldsymbol{h}$ is the channel vector of length $L+1, \boldsymbol{x}^*$ is the transmitted symbol sequence of length N, and $\boldsymbol{n}$ is an additive noise matrix whose elements are assumed to be i.i.d. complex Gaussian random variables. We also assume that the entries of $\boldsymbol{x}^*$ are i.i.d. symbols drawn from a certain constellation Ω (like BPSK or 16-QAM). We can write (4.1) in matrix form as

$$\boldsymbol{y} = \boldsymbol{X}\boldsymbol{h} + \boldsymbol{n} \tag{3.2}$$

where $\boldsymbol{X}$ is the data matrix which has a rectangular Toeplitz structure, i.e., it has constant entries along its diagonals.

$$\boldsymbol{X} = \begin{bmatrix} x(1) & 0 & 0 & 0 & \cdots & 0 \\ x(2) & x(1) & 0 & 0 & \cdots & 0 \\ x(3) & x(2) & x(1) & 0 & \cdots & 0 \\ \vdots & \ddots & \ddots & \ddots & \ddots & 0 \\ x(N) & x(N-1) & \cdots & \cdots & x(N-L+1) & x(N-L) \end{bmatrix}_{N \times L+1}$$

Note that each row of $\boldsymbol{X}$ amounts to a state vector (also called a regressor) of the channel. Specifically, the ith row of $\boldsymbol{X}$ has the form

$$\boldsymbol{x}_i^* = [\ x(i)\ \ x(i-1)\ \ ...\ \ x(i-L-1)\ ]$$

which contains the input at time $i, x(i)$, as well as the outputs of all delay elements in the channel.

3.3 Blind Equalization Approach

The problem of joint ML channel estimation and data detection for SISO channels is transformed into the following optimization problem

$$J = \min_{h, x \in \Omega^N} \|\boldsymbol{y} - \boldsymbol{X}\boldsymbol{h}\|^2 \tag{3.3}$$

where Ω^N denotes the set of N-dimensional signal vector.

Let us consider a partial data sequence $\boldsymbol{x}^*_{(i)}$ up to the time index i, i.e.

$$\boldsymbol{x}^*_{(i)} = [x(1) \quad x(2) \quad \cdots \quad x(i)]$$

Alternatively, we let $\boldsymbol{X}_{(i)}$ denote the matrix that consists of the first$i$ rows of $\boldsymbol{X}$, i.e.

$$\boldsymbol{X}_{(i)} = \begin{bmatrix} x(1) & 0 & 0 & \cdots & 0 \\ x(2) & x(1) & 0 & \cdots & 0 \\ \vdots & \ddots & \ddots & \ddots & 0 \\ x(i) & x(i-1) & \cdots & x(i-L+1) & x(i-L) \end{bmatrix}$$

Now define $M_{x^*_{(i)}}$ to be the cost function associated with the first i data symbols, i.e.

$$M_{x^*_{(i)}} = \|\boldsymbol{y}_{(i)} - \boldsymbol{X}_{(i)}\boldsymbol{h}\|^2 \tag{3.4}$$

Now, as per Weiyu's paper [97], let R be the optimal value for our objective function in (3.3), if $M_{x^*_{(i)}} > R$, then $\boldsymbol{x}^*_{(i)}$ can not be the first i symbols of the ML solution $\hat{\boldsymbol{x}^*}_{(i)}$ to (3.3).

To prove this, suppose $\hat{\boldsymbol{x}}^*_{(i)} = \boldsymbol{x}^*_{(i)}$ and $\hat{\boldsymbol{X}}_{(i)} = \boldsymbol{X}_{(i)}$, and denote the optimal channel gain corresponding to $\hat{\boldsymbol{x}}^*_{(i)}$ as $\hat{\boldsymbol{h}}$. Then

$$
\begin{aligned}
R &= \|\boldsymbol{y}_{(i)} - \hat{\boldsymbol{X}}_{(i)}\hat{\boldsymbol{h}}\|^2 + \sum_{j=i+1}^{N} |y(j) - \hat{\boldsymbol{X}}_j\hat{\boldsymbol{h}}|^2 && (3.5)\\
&\geq \min_h \|\boldsymbol{y}_{(i)} - \hat{\boldsymbol{X}}_{(i)}\boldsymbol{h}\|^2 + \sum_{j=i+1}^{N} |y(j) - \hat{\boldsymbol{X}}_j\hat{\boldsymbol{h}}|^2 && (3.6)\\
&\geq \min_h \|\boldsymbol{y}_{(i)} - \hat{\boldsymbol{X}}_{(i)}\boldsymbol{h}\|^2 = M_{\hat{x}^*_{(i)}} = M_{x^*_{(i)}} && (3.7)
\end{aligned}
$$

where $\boldsymbol{X}_j$ corresponding to exactly the Jth row of $\boldsymbol{X}$.

So, for $\boldsymbol{x}_{(i)}$ to correspond to the first i symbols of the ML solution $\hat{\boldsymbol{x}}_{(i)}$, we should have $M_{x^*_{(i)}} < R$. Note that the above represents a necessary condition only in that if $\hat{\boldsymbol{x}}_{(i)}$ is such that $M_{x^*_{(i)}} < R$, then that does not necessarily mean that $\hat{\boldsymbol{x}}_{(i)}$ coincides with $\boldsymbol{x}_{(i)}$. In the next subsection (3.3.1), we will use this properly in our blind algorithm.

Since $\boldsymbol{h}$ has $L+1$ degrees of freedom, so we need $L+1$ pilots to identify it. Alternatively, we need to make a guess of $L+1$ consecutive values of the input before we get a unique solution for $\boldsymbol{h}$. In otherwords, with $i < L+1$, it is always possible to choose $\hat{\boldsymbol{X}}_i$ and $\hat{\boldsymbol{h}}$ so that the cost function in (3.4) is identically zero. This does not allow us to refine our search to obtain the most suitable data sequence.

To avoid this problem, we replace the cost function in (3.3) with the regularized least squares problem

$$
J = \min_{h,x\in\Omega^N} \|\boldsymbol{h}\|^2_{R_h^{-1}} + \|\boldsymbol{y} - \boldsymbol{X}\boldsymbol{h}\|^2_{Rn^{-1}} \qquad (3.8)
$$

where $\boldsymbol{R}_h$ is the autocorrelation matrix of $\boldsymbol{h}$ and $\boldsymbol{R}_n$ is the noise autocorrelation matrix, given by $\sigma^2\boldsymbol{I}$ where σ^2 is the noise variance. In this case, we can show that

$M_{x^*_{(i)}}$ is given by

$$M_{x^*_{(i)}} = \|\boldsymbol{h}\|^2_{R_h^{-1}} + \|\boldsymbol{y}_{(i)} - \boldsymbol{X}_{(i)}\boldsymbol{h}\|^2_{Rn^{-1}} \quad (3.9)$$

$$= \boldsymbol{y}^*_{(i)}[\boldsymbol{R}_n + \boldsymbol{X}^*_{(i)}\boldsymbol{R}_h\boldsymbol{X}_{(i)}]^{-1}\boldsymbol{y}_{(i)} \quad (3.10)$$

This solution is computationally complex as it use the *matrix inversion lemma*. So, we can recursively calculate the value of the objective function ($M_{x^*_{(i)}}$) for each i using the RLS algorithm through the following set of recursions

$$\boxed{M_{x^*_{(i)}} = M_{x^*_{(i-1)}} + \tfrac{1}{\sigma^2}\gamma(i)|y(i) - \boldsymbol{x}_i^*\hat{\boldsymbol{h}}_{i-1}|^2} \quad (3.11)$$

where

$$\boxed{\hat{\boldsymbol{h}}_i = \hat{\boldsymbol{h}}_{i-1} + \tfrac{1}{\sigma}\boldsymbol{g}_i(y(i) - \boldsymbol{x}_i^*\hat{\boldsymbol{h}}_{i-1})} \quad (3.12)$$

and

$$\boldsymbol{g}_i = \frac{1}{\sigma}\gamma(i)\boldsymbol{P}_{i-1}\boldsymbol{x}_i \quad (3.13)$$

$$\gamma(i) = \frac{1}{1 + \frac{1}{\sigma^2}\boldsymbol{x}_i^*\boldsymbol{P}_{i-1}\boldsymbol{x}_i} \quad (3.14)$$

$$\boldsymbol{P}_i = \boldsymbol{P}_{i-1} - (\boldsymbol{g}_i\boldsymbol{g}_i^*)/\gamma(i) \quad (3.15)$$

$$= \boldsymbol{P}_{i-1} - \frac{1}{\sigma^2}\gamma(i)\boldsymbol{P}_{i-1}\boldsymbol{x}_i\boldsymbol{x}_i^*\boldsymbol{P}_{i-1} \quad (3.16)$$

These recursions apply for all i and are initialized by

$$M_{x^*_{(-1)}} = 0, \quad \boldsymbol{P}_{-1} = \boldsymbol{R}_h, \quad \text{and} \quad \hat{\boldsymbol{h}}_{-1} = \boldsymbol{0}$$

Now, R is the optimal value for the regularized objective function in (3.8), and $M_{x^*_{(i)}}$ is the value of the objective function in (3.11) for the sequence $\boldsymbol{x}^*_{(i)}$ up to the time index i. If the value R can be estimated, we can restrict the search of the blind ML solution $\hat{\boldsymbol{x}}^*$ to the offsprings of those partial sequences $\boldsymbol{x}^*_{(i)}$ which satisfy $M_{x^*_{(i)}} < R$.

3.3.1 Exact Blind Algorithm

In this section, we describe the algorithm that we use to find the ML solution of the system input from the output observations. The algorithm employs the above set of iterations (3.11)−(3.16) to update the value of the cost function ($M_{x^*_{(i)}}$) which we need for the comparison with the estimated value R (we denote it in the blind algorithm below as the search radius r).

The input parameters for this algorithm are:

- The received channel output $\boldsymbol{y}$
- The search radius r
- The modulation constellation Ω
- $1 \times N$ index vector I

We denote the kth constellation point in the modulation constellation Ω as $\Omega(k)$.

The following steps explain the process of our algorithm, which were illustrated in the flowchart (Figure 2.1) in the previous chapter:

1. Set $i = 1$, $r_i = r$, $I(i) = 1$ and set $x(i) = \Omega(I(i))$.

2. (Computing the bounds) Compute the metric $M_{x^*_{(i)}}$ using the equation (3.11). If $M_{x^*_{(i)}} > r$, go to 3; else, go to 4;

3. (Backtracking) Find the largest $1 \leq j \leq i$ such that $I(j) < |\Omega|$. If there exists such j, set $i = j$ and go to 5; else go to 6.

4. If $i = N$, store current $\boldsymbol{x}^*_{(N)}$, update $r = M_{x^*_{(N)}}$ and go to 3; else set $i = i + 1, I(i) = 1$ and $x(i) = \Omega(I(i))$, go to 2.

5. Set $I(i) = I(i) + 1$ and $x(i) = \Omega(I(i))$. Go to 2.

6. If any sequence $\boldsymbol{x}^*_{(N)}$ is ever found in Step 4, output the latest stored full-length sequence as ML solution; otherwise, double r and go to 1.

3.4 Reducing the Computational Complexity

In the previous chapter, we have mentioned two drawbacks to the blind backtracking algorithm, namely: (1) the need for backtracking and (2) calculating the $(L+1) \times (L+1)$ matrix $\boldsymbol{P}_i$. In the following, we get over the second drawback by avoiding the need to calculate $\boldsymbol{P}_i$ while in the next section we will get over the first drawback by suggesting a new method to avoid the backtracking operation.

The RLS algorithm that we have used above is not assume any structure in the data. So, the computational complexity of this algorithm is $O((L+1)^2)$ operations per iteration (see table 3.1), where $L+1$ is the channel length. However, when data structure is present, more efficient implementations are possible.

In our case (Linear systems), the regressors $\boldsymbol{x}_i^*$ exhibit some form of structure which arise as regressors of a tapped-delay-line implementation. That is, we can see that the entries of $\boldsymbol{x}_i^*$ are formed from time-delayed samples of an input sequence $x(.)$, say,

$$\boldsymbol{x}_i^* = [\ x(i)\ \ x(i-1)\ \ ...\ \ x(i-L-1)\ \ ]$$

The shift structure in the regressors allows us to utilize an efficient recursive least-squares solutions, which is the Fast RLS Array Algorithm. By efficient we mean its computational complexity is $O(L+1)$ operations per iteration, as opposed to $O((L+1)^2)$.

So, we can recursively calculate the value of the objective function in (3.9) (reproduced here for convenience)

$$M_{x^*_{(i)}} = \|\boldsymbol{h}\|^2_{R_h^{-1}} + \|\boldsymbol{y}_{(i)} - \boldsymbol{X}_{(i)}\boldsymbol{h}\|^2_{Rn^{-1}} \tag{3.17}$$

for each i using the Fast RLS array algorithm through the following set of recursions initialized by

$$M_{x^*_{(-1)}} = 0, \quad \boldsymbol{g}_{-1} = 0, \quad \gamma^{-1/2}(-1) = 1, \quad \hat{\boldsymbol{h}}_{-1} = \mathbf{0},$$

$$\boldsymbol{L}_{-1} = \sqrt{\eta\lambda}\begin{bmatrix} 1 & 0 \\ 0 & 0 \\ \vdots & \vdots \\ 0 & 0 \\ 0 & \lambda^{(L+1)/2} \end{bmatrix}, \quad \boldsymbol{S}_{-1} = \begin{bmatrix} 1 & 0 \\ 0 & -1 \end{bmatrix} \text{ and } l = \text{diag}(1, \boldsymbol{S})$$

where $\boldsymbol{L}_{-1}$ is $((L+2) \times 2)$ matrix and $\boldsymbol{S}_{-1}$ is (2×2) signature matrix.

1. Find the $l-$unitary matrix Θ_i that annihilates the last two entries in the top row of the post-array below and generates a positive leading entry. The $l-$unitary matrix Θ should satisfy

$$\Theta \begin{bmatrix} 1 & \\ & \boldsymbol{S} \end{bmatrix} \Theta^* = \begin{bmatrix} 1 & \\ & \boldsymbol{S} \end{bmatrix}$$

   Then the entries of the post-array will correspond to

$$\begin{bmatrix} \gamma^{-1/2}(i-1) & [x(i) \quad \boldsymbol{x}_{i-1}]\,\boldsymbol{L}_{i-1} \\ \begin{bmatrix} 0 \\ \boldsymbol{g}_{i-1}\gamma^{-1/2}(i-1) \end{bmatrix} & \boldsymbol{L}_{i-1} \end{bmatrix} \Theta_i$$

$$= \begin{bmatrix} \gamma^{-1/2}(i) & [0 \quad 0] \\ \begin{bmatrix} \boldsymbol{g}_i\gamma^{-1/2}(i) \\ 0 \end{bmatrix} & \sqrt{\lambda}\boldsymbol{L}_i \end{bmatrix}$$

2. Update the channel

$$\boxed{\hat{\boldsymbol{h}}_i = \hat{\boldsymbol{h}}_{i-1} + \frac{1}{\sigma}\left[\boldsymbol{g}_i\gamma^{-1/2}(i)\right]\left[\gamma^{-1/2}(i)\right]^{-1}\left(y(i) - \boldsymbol{x}_i^*\hat{\boldsymbol{h}}_{i-1}\right)} \tag{3.18}$$

where the quantities $\{\boldsymbol{g}_i\gamma^{-1/2}(i), \gamma^{-1/2}(i)\}$ are read from the post-array.

3. Update the cost function in (3.17)

$$\boxed{M_{x^*_{(i)}} = M_{x^*_{(i-1)}} + \frac{1}{\sigma^2}\gamma(i)|y(i) - \boldsymbol{x}_i^*\hat{\boldsymbol{h}}_{i-1}|^2}$$

We know that $\boldsymbol{R}_h$ is the autocorrelation matrix of $\boldsymbol{h}$, but here in this algorithm, it should has the form

$$\boldsymbol{R}_h^{-1} = \eta \ \text{diagonal}(\lambda^2, \lambda^3, \ldots, \lambda^{L+2})$$

where η is a positive scalar (usually large) and λ is the forgetting factor ($0 \ll \lambda \leq 1$).

Observe that this array algorithm computes the gain vector $\boldsymbol{g}_i$ without evaluating the $(L+1)\times(L+1)$ matrix $\boldsymbol{P}_i$. Instead, the low-rank factor $\boldsymbol{L}_i$, which is $(L+2)\times 2$, is propagated, resulting in a lower computational complexity. In section 3.6, Table (3.1), we shall compare the computational complexity for this fast array algorithm and the RLS algorithm.

3.5 Minimum Cost Method

In the previous section, we showed how to avoid the need for calculating $\boldsymbol{P}_i$ by using the Fast RLS algorithm. In this section, we propose a new method to avoid the backtracking operation in the blind algorithm and give a very low complexity.

Our objective in data detection is to minimize the cost function. In this method, we depend on finding the constellation points that minimize the cost function at each data symbol (according to the following equation (3.19)) and take them as a solution without the need for backtracking.

From (3.11), and for the j-th constellation point $(\Omega(j))$, we can define $M^{j}_{x^*_{(i)}}$ as the cost function up to the time index i, say

$$\boxed{M^{j}_{x^*_{(i)}} = M_{x^*_{(i-1)}} + \frac{1}{\sigma^2}\gamma(i)|y(i) - \Omega(j)\hat{\boldsymbol{h}}_{i-1}|^2} \tag{3.19}$$

After we compute all the j values of the cost function using the above equation, we find the minimum one and its index (l), then store the l-th constellation point in the i-th solution $\hat{x}(i)$. The same procedure is followed for the next symbol up to the one at time N.

In this method, there is no need to do backtracking, which gives us a very low complexity compared with the backtracking method in Section 3.3.1, but this method needs to have some pilots to give good results as we shall show in the simulation results.

In addition, this method can be also used as an equalization method when the receiver has perfect or estimated knowledge of channel.

3.6 Computational Complexity Comparison

In this section, we provide a comparison of our blind algorithm and the two approximate methods. Table 3.1 lists the estimated computational cost per iteration for the blind algorithm using RLS and Fast RLS and for the minimum cost method, assuming real data. The costs are in terms of the number of multiplications and additions that are needed for each iteration. Here, k is the length of the channel, N is the length of the data sequence and m is the size of the symbol alphabet.

We assume that the computational cost of the blind algorithm described in Subsection 3.3.1 as a function of N per iteration ($f(N)$), thus the computational complexity of the blind RLS and fast RLS algorithms will be multiplied by this function because the blind algorithm needs to compute the cost function $M_{x^*_{(i)}}$ using the RLS or fast RLS algorithm for each backtracking operation.

The minimum cost method computes the cost function ($M_{x^*_{(i)}}$) m times per iteration using the RLS algorithm. So, its computational cost will be m times the computational cost of the RLS algorithm.

It is seen from Table 3.1 that the blind RLS algorithm requires ($O(k^2)f(N)$) operations per iteration, while when we use the fast RLS instead of it in the same blind algorithm, the computational cost reduced to ($O(k)f(N)$) operations per iteration.

Table 3.1: Computational cost comparison for SISO blind algorithms

Algorithm	$\times$	$+$
Blind RLS algorithm	$(4k^2+5k+4)f(N)$	$(3k^2+1)f(N)$
Blind Fast-RLS algorithm	$(6k+4)f(N)$	$(10k+16)f(N)$
Minimum cost method	$(4k^2+5k+4)m$	$(3k^2+1)m$

3.7 Simulation Results

This section is divided into two parts. In the first part, simulation results of the blind equalization are discussed while in the second part, we provide results for the approximate methods.

3.7.1 Blind Equalization

In this subsection, we show simulation results for the performance of our blind algorithm. We investigate its performance in SISO system employing BPSK, 4QAM and 16QAM modulation. We compare our results with the equalization of the perfect channel case. We do so using the backtracking algorithm because the linear equalization techniques don't give good results and so the comparison would not be fair.

BER vs SNR Comparison for BPSK Modulated Data

In Figure 3.1, we assume a packet of $N = 30$ data symbols and a channel IR of 5 taps iid complex Gaussian random variables which remain constant over one packet. We compare the new blind algorithm with the case of perfect known channel for BPSK modulated data over a Rayleigh fading channel. As we see, the blind detection algorithm shows performance that is very close to the perfectly known channel case at high SNR.

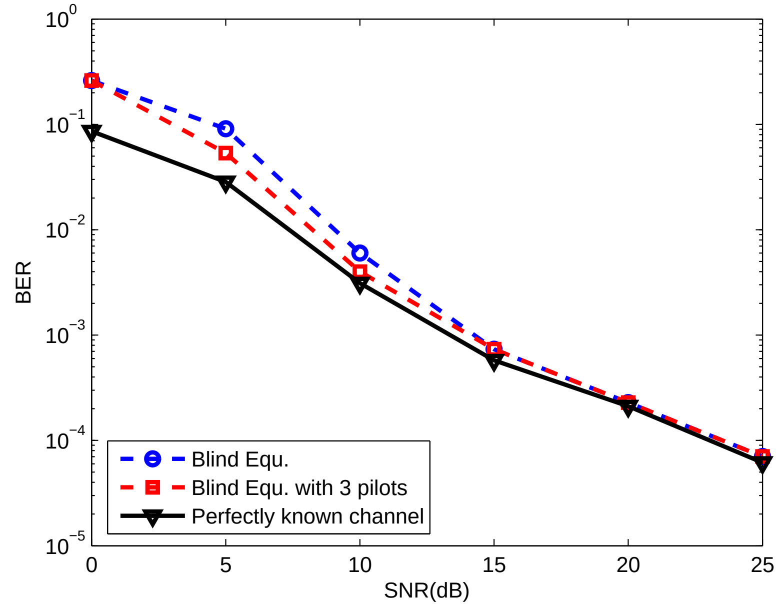

Figure 3.1: BER vs SNR for BPSK-SISO over a Rayleigh channel

BER vs SNR Comparison for QAM Modulated Data

For 4QAM and 16QAM modulation, we assume a packet of $N = 16$ data symbols and a rayleigh fading channel IR of 4 taps which remain constant over one packet. Figure 3.2 and 3.3 show a comparison between our blind algorithm with and without using pilots and the perfectly known channel for 4QAM and 16QAM input data respectively, where our algorithm shows favorable BER performance in both scenarios. We can see here also that the pilots don't add much to improve the performance.

3.7.2 Approximate Methods

In this subsection, we demonstrate the simulation results of the two approximate methods. We consider the same SISO systems used in the previous section for BPSK and QAM input data. To setup the Fast RLS algorithm we used a forgetting factor

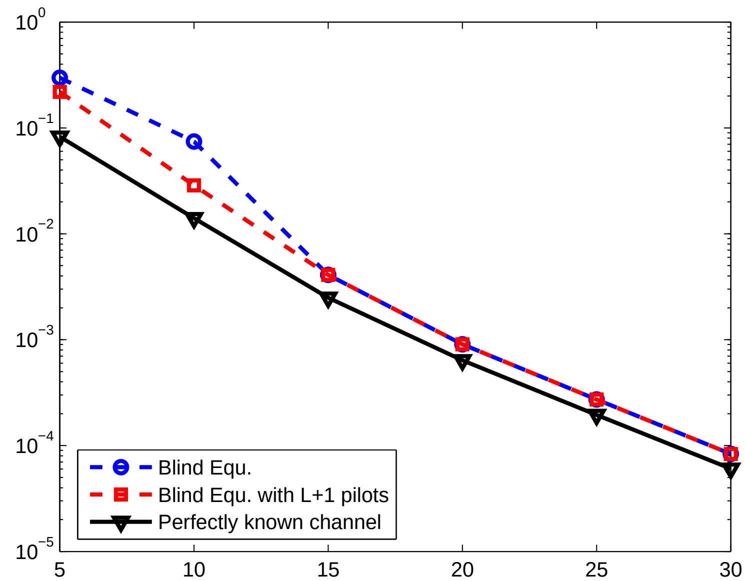

Figure 3.2: BER vs SNR for 4QAM-SISO over a Rayleigh channel

of $\lambda = 0.999$ and $\eta = 5$.

Performance of low complexity algorithms for BPSK Modulated Data

Figure 3.4 shows the BER performance comparison between the backtracking method and the low computational complexity method (Fast RLS algorithm), for BPSK input data. As we see the method of low complexity performs very close to the blind RLS method.

Performance of low complexity algorithms for 4QAM Modulated Data

The BER performance of the backtracking method and the low computational complexity method is given in Figure 3.5, for 4QAM input data. Our conclusion is similar to the conclusion in the BPSK case, namely, the Fast RLS algorithm performs very

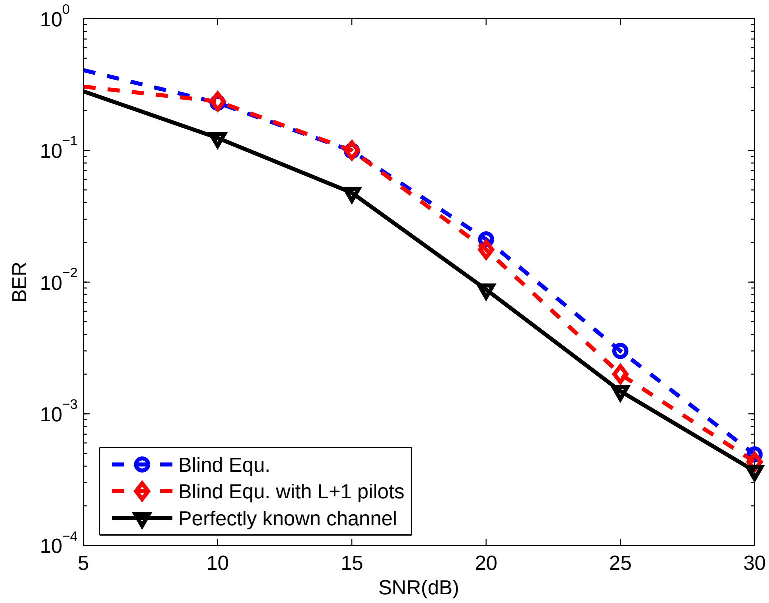

Figure 3.3: BER vs SNR for 16QAM-SISO over a Rayleigh channel

closely to the performance of the RLS backtracking method.

Performance of the minimum cost method for BPSK Modulated Data

In Figure 3.6, we show the performance of the minimum cost method for BPSK input data with $N = 30$ over 5 Rayleigh fading channel taps. We investigate its performance for three cases; using one training symbol, using $L + 1$ pilots and using the perfectly known channel. The case of perfectly known channel gives, as expected, the best performance. Therefore, we conclude that the minimum cost method is best suited for the equalization of perfectly known channel.

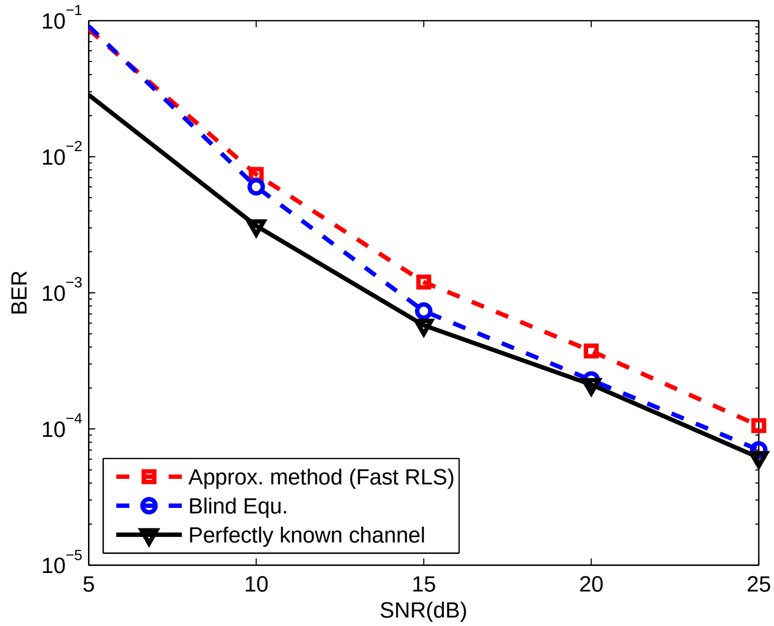

Figure 3.4: Performance of low complexity algorithm for BPSK-SISO

Performance of minimum cost method for QAM Modulated Data

Figure 3.7 and 3.8, show the performance of the minimum cost method for 4QAM and 16QAM input data, respectively, with $N = 16$ over a Rayleigh fading channel with 4 taps. The same conclusion of BPSK case can be made here, namely, that the minimum cost method is best suited for equalization of perfectly known channel.

3.8 Conclusion

In this chapter, we proposed a new blind algorithm for data detection in SISO wireless systems employing data with general constellation. The algorithm is able to recover the data from the output observations only. Simulation results showed the favorable performance of the algorithm for several constellations (BPSK, 4QAM and 16QAM).

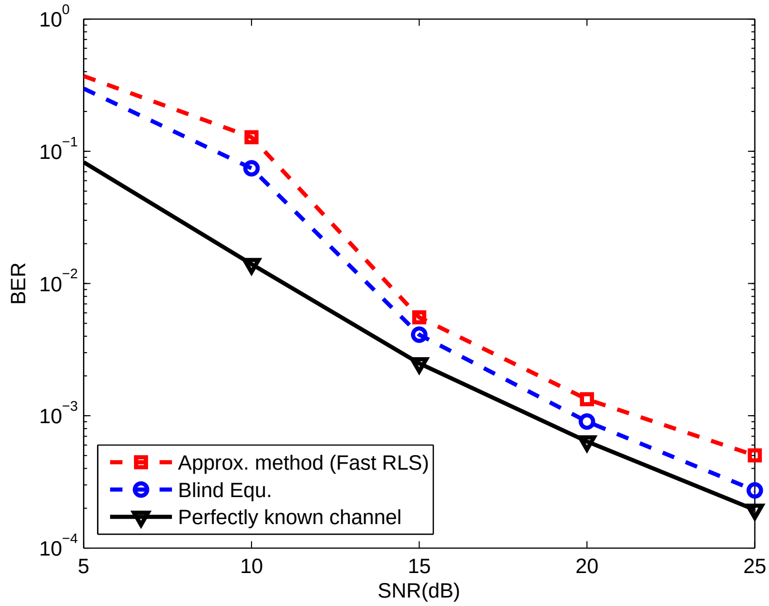

Figure 3.5: Performance of low complexity algorithm for 4QAM-SISO

Also, we showed that using pilots didn't add much improvement to the performance of the algorithm (which allows us to increase the throughput without affecting the performance).

We have also proposed approximate methods to reduce the complexity entailed in the algorithm developed in the chapter. The regressors $\boldsymbol{x}_i^*$ in SISO systems exhibit some form of structure which arise as regressors of a tapped-delay-line implementation. This allowed us to use the Fast RLS algorithm which allows us to avoid the need for calculating the matrix $\boldsymbol{P}_i$ in the blind RLS algorithm, reducing the computational complexity drastically. As is evident from the simulation results, these approximate methods perform quite close to the original blind algorithm.

A new equalization method (minimum cost method) was also proposed, when the receiver has perfect or estimated knowledge of channel.

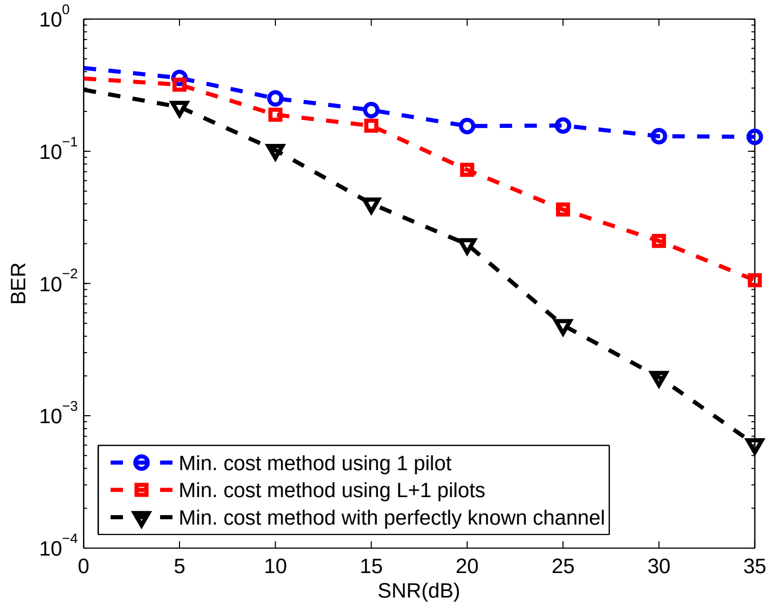

Figure 3.6: Performance of minimum cost method for BPSK-SISO over a Rayleigh channel

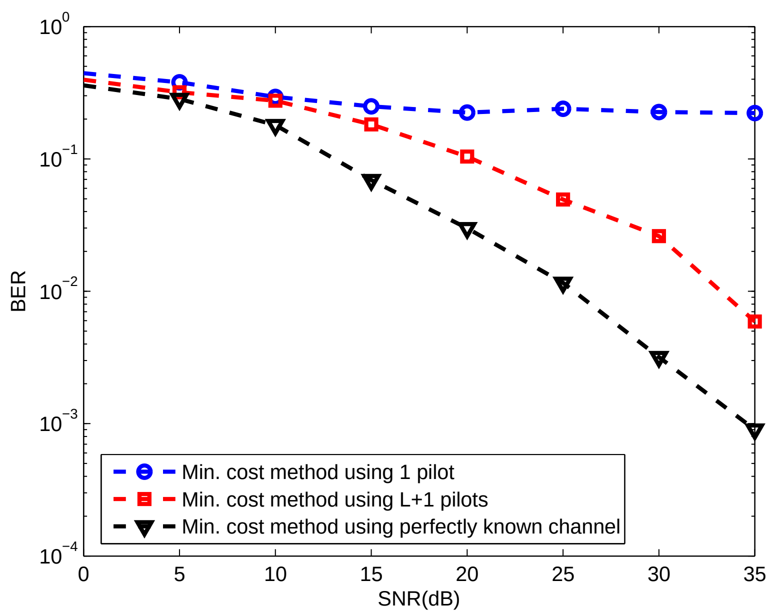

Figure 3.7: Performance of minimum cost method for 4QAM-SISO over a Rayleigh channel

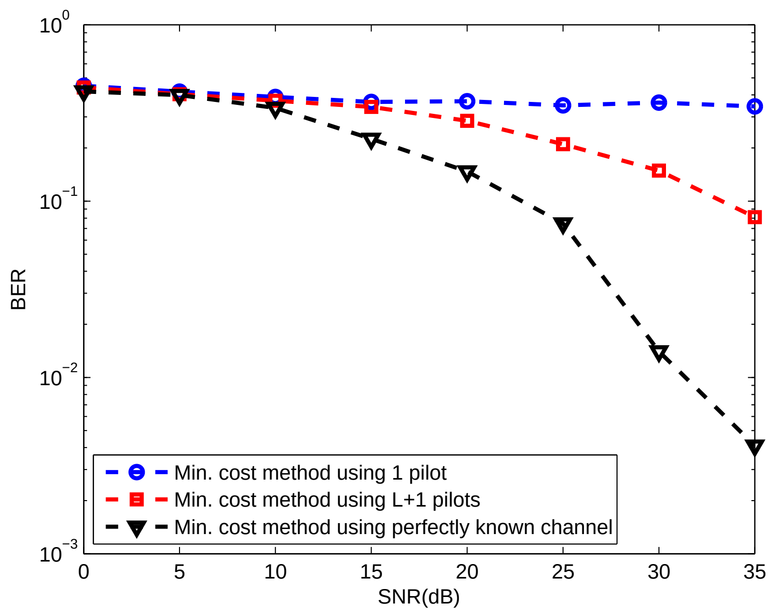

Figure 3.8: Performance of minimum cost method for 16QAM-SISO over a Rayleigh channel

CHAPTER 4

SISO SYSTEMS OVER TIME-VARIANT CHANNELS

4.1 Introduction

The goal of achieving high-speed reliable data transmission over highly dynamic wireless medium has generated a lot of research activities in the communications and signal processing community. One of the largest challenges arising in wireless communications is how to deal with the wireless fading phenomenon, where the wireless channels may vary over time. In wireless communications, one often assumes knowledge of the channel coefficients at the receiver side by channel estimation from training sequences, but sending training symbols will sacrifice a fraction of the transmission rate. In wireless mobile systems, the channels may even change so rapidly that training and channel tracking will become infeasible. One possible solution is to differentially encode the transmitted data and thus eliminate the need for channel knowledge. Another solution is to do blind or semi-blind detection over the time-varying wireless channels, which has been shown to enhance the system performance considerably and often perform better than differential modulations.

In this chapter, we consider the problem of joint maximum likelihood (ML) channel estimation and data detection for linear convolution SISO systems over time-variant channels.

4.1.1 The Approach and Organization of this Chapter

This chapter considers blind receiver design for linear convolution SISO transmission over frequency selective time-variant channels. The receiver employs the ML algorithm for joint channel and data recovery. It makes collective use of the data and channel constraints that characterize the communication problem. The data constraints include the finite alphabet constraint. The channel constraints include the finite delay spread and frequency and time correlation.

We perform data identification and equalization from output observations only, without the need for a training sequence or a priori channel information. The advantage of our approach is three fold:

1. The method provides a *blind detection* of the data from one output data packet without the need for training.

2. The algorithm works on linear convolution SISO systems employing data with *general constellations*.

3. The algorithm works on linear convolution SISO systems over *time-variant channel* without any restriction.

This chapter is organized as follows. We give a description of the channel model in Section 4.2. Section 4.3 then presents our approach, and Section 4.4 demonstrates our simulations. We conclude the chapter in Section 4.5.

4.2 Channel Model

In the previous chapter, we have described our algorithm using block fading channels, which showed a favorable results. In this chapter, we peruse the same backtracking algorithm in time variant channels.

Let us consider the same SISO system in the previous chapter, where the input/output relationship can be written as

$$\begin{aligned} \boldsymbol{y} &= \boldsymbol{h} * \boldsymbol{x}^* + \boldsymbol{n} && (4.1) \\ &= \boldsymbol{X}\boldsymbol{h} + \boldsymbol{n} && (4.2) \end{aligned}$$

except that the channel vector $\boldsymbol{h}$ of length $L+1$ varies here from one symbol to the next according to the following state space model

$$\boldsymbol{h}_{i+1} = \boldsymbol{F}\boldsymbol{h}_i + \boldsymbol{G}\boldsymbol{u}_i \tag{4.3}$$

where $\boldsymbol{h}_0 \sim \boldsymbol{\mathcal{N}}(0, \boldsymbol{R})$ and $\boldsymbol{u}_i \sim \boldsymbol{\mathcal{N}}(0, \sigma_u^2 I)$. The matrices $\boldsymbol{F}$ and $\boldsymbol{G}$ in (4.3) are square matrices of size $L+1$ and are function of Doppler spread, power delay profile and transmit filter, and they are given by

$$\boldsymbol{F} = \begin{bmatrix} \alpha(0) & & & \\ & \alpha(1) & & \\ & & \ddots & \\ & & & \alpha(L) \end{bmatrix} \quad \text{and}$$

$$\boldsymbol{G} = \begin{bmatrix} \sqrt{1-\alpha^2(0)} & & & \\ & \sqrt{(1-\alpha^2(1))e^{-\beta(1)}} & & \\ & & \ddots & \\ & & & \sqrt{(1-\alpha^2(L))e^{-\beta L}} \end{bmatrix}$$

where $\alpha(l)$ is related to the Doppler frequency $f_D(l)$ by $\alpha(l) = J_0(2\pi f_D(l)T)$, where J_0 denotes the zero-order Bessel function of the first kind and T is the symbol time. The variable β corresponds to the exponent of the channel decay profile while the factor $\sqrt{(1-\alpha^2(l))e^{-\beta l}}$ ensures that each link maintains the exponential decay profile ($e^{-\beta l}$) for all time.

The Doppler frequency $f_D(l)$ is related to the vehicle speed $v(l)$ and the wavelength $\lambda = \frac{c}{f}$ by $f_D(l) = \frac{v(l)}{\lambda}$, where c is the speed of light and f is the transmission frequency. In our simulations, we consider constant vehicle speed, i.e. $v(l) = v$, thus the time variation parameter α become constant and the matrices $\boldsymbol{F}$ and $\boldsymbol{G}$ will given by

$$\boldsymbol{F} = \alpha \boldsymbol{I} \quad \text{and} \quad \boldsymbol{G} = \begin{bmatrix} \sqrt{1-\alpha^2} & & & \\ & \sqrt{(1-\alpha^2)e^{-\beta(1)}} & & \\ & & \ddots & \\ & & & \sqrt{(1-\alpha^2)e^{-\beta L}} \end{bmatrix}$$

4.3 Blind Equalization Approaches

In this section, we describe the problem of time variant channel from two aspects. In the first aspect, we consider the time variation case without assuming that the dynamical relation (4.3) is available. In this case, we pursue two methods for blind equalization. In the first method, we use the same solution of the time invariant channel case as in the previous chapter with additional diagonal weighting matrix whose purpose is to give more weight to recent data and less weight to data from the remote past. In the second method, we use the Fast RLS algorithm that we have used in the previous chapter to reduce the complexity.

In the second aspect, we assume that the dynamical model (4.3) is available to the receiver. Here, we can apply the Extended RLS algorithm that are better suited for tracking the state-vector of general linear Dynamical models as in (4.3).

4.3.1 Blind Equalization Without Knowledge of the Channel's Dynamical Model

In this subsection, we consider the case of no knowledge of the matrices $\boldsymbol{F}$ and $\boldsymbol{G}$ in the dynamical model (4.3) are available at the receiver. We pursue here two methods for blind equalization described below.

Exponentially-Weighted RLS Approach

In our first approach, we use an Exponentially-Weighted RLS algorithm. Here, we employ a weighted regularized least-squares cost function, as opposed to the unweighted cost in (3.8). Namely, replace the cost function in (3.8) by

$$J = \min_{h,x\in\Omega^N}\left[\|\boldsymbol{h}\|^2_{\lambda^N R_h^{-1}} + \|\boldsymbol{y}-\boldsymbol{X}\boldsymbol{h}\|^2_{\Lambda^{-1}}\right] \tag{4.4}$$

where $0 \ll \lambda < 1$ is a positive scalar, usually very close to one, and introduce the diagonal matrix

$$\Lambda = \text{diag}\{\lambda^{N-1},\ \ \lambda^{N-2},\ \ \ldots,\ \ \lambda,\ \ 1\}$$

The scalar λ is called the *forgetting factor* since past data are weighted less heavily than more recent data. The special case $\lambda = 1$ is known as the *growing memory* case and it was studied in the previous chapter.

Observe that the regularization matrix in (4.4) is chosen as $\lambda^N \boldsymbol{R}_h^{-1}$, with the additional scaling factor λ^N. Since this factor becomes smaller as time progresses, we see that the exponentially-weighted cost function (4.4) is such that it de-emphasizes regularization during the later stages of operation when the data matrix $\boldsymbol{X}$ is more likely to have full rank.

Here, the solution $\boldsymbol{h}$ of the exponentially-weighted regularized least-squares problem (4.4), and the corresponding minimum cost J, can be computed recursively as follows [92]. Start with

$$J_{(-1)} = 0, \quad \boldsymbol{P}_{-1} = \boldsymbol{R}_h, \quad \text{and} \quad \hat{\boldsymbol{h}}_{-1} = \boldsymbol{0}$$

and iterate for $i \geq 0$:

$$\boxed{J_{(i)} = \lambda J_{(i-1)} + \gamma(i)|y(i) - \boldsymbol{x}_i^* \hat{\boldsymbol{h}}_{i-1}|^2} \tag{4.5}$$

$$\boxed{\hat{\boldsymbol{h}}_i = \hat{\boldsymbol{h}}_{i-1} + \boldsymbol{g}_i(y(i) - \boldsymbol{x}_i^* \hat{\boldsymbol{h}}_{i-1})} \tag{4.6}$$

where

$$\boldsymbol{g}_i = \lambda^{-1}\gamma(i)\boldsymbol{P}_{i-1}\boldsymbol{x}_i \tag{4.7}$$

$$\gamma(i) = 1/(1 + \lambda^{-1}\boldsymbol{x}_i^* \boldsymbol{P}_{i-1}\boldsymbol{x}_i) \tag{4.8}$$

$$\boldsymbol{P}_i = \lambda^{-1}\boldsymbol{P}_{i-1} - (\boldsymbol{g}_i\boldsymbol{g}_i^*)/\gamma(i) \tag{4.9}$$

and $J_{(i)}$ is the cost function up to the time index i.

Now, after we compute the value of the cost function, we can employ the backtracking algorithm introduced in Section 3.3.1 of the previous chapter to estimate the channel and detect the transmitted data blindly.

Fast RLS Approach

In our second approach, We employ the same Fast RLS algorithm used in the previous chapter where we have used it to reduce the computational complexity involved in the RLS backtracking algorithm by avoiding the need for calculating the matrix $\boldsymbol{P}_i$. Here, in addition to this advantage, we use this algorithm to track the channel and time diversity, where the same recursions in Section 3.4 can be used to compute the cost function $M_{x^*_{(i)}}$ needed in the backtracking method (see Section 3.3.1) to detect the transmitted data blindly.

4.3.2 Blind Equalization Using the Channel's Dynamical Model Information

In this subsection, we assume that the matrices $\boldsymbol{F}$ and $\boldsymbol{G}$ in the dynamical model (4.3) are known to the receiver. Here, we can apply the Extended RLS algorithm that are better suited for tracking the state-vector of general linear Dynamical models.

Extended RLS Approach

Consider the dynamical channel model (4.3). We pose the problem of estimating the state vector $\boldsymbol{h}$ in a regularized least-squares manner by solving

$$J = \min_{h, X \in \Omega^N} \left[\|\boldsymbol{h}\|^2_{R_h^{-1}} + \|\boldsymbol{y} - \boldsymbol{X}\boldsymbol{h}\|^2_{R_n^{-1}} + \|\boldsymbol{u}\|^2_{R_u^{-1}} \right] \tag{4.10}$$

where $\boldsymbol{R}_u$ and $\boldsymbol{R}_n$ are positive-definite weighting matrices that could be taken as the covariance matrices of the noises $\boldsymbol{u}$ (i.e. $\sigma_u^2\boldsymbol{I}$) and $\boldsymbol{n}$ (i.e. $\sigma_n^2\boldsymbol{I}$), respectively.

The solution $\boldsymbol{h}$ and the cost function J can be determined recursively as follows [92]. Start with

$$J_{(-1)} = 0, \quad \boldsymbol{P}_{-1} = \boldsymbol{R}_h, \quad \text{and} \quad \hat{\boldsymbol{h}}_{-1} = \boldsymbol{0}$$

and run the following equations for $i \geq 0$:

$$\boxed{J_{(i)} = J_{(i-1)} + \gamma(i)^{-1}|y(i) - \boldsymbol{x}_i^*\hat{\boldsymbol{h}}_{i-1}|^2} \tag{4.11}$$

$$\boxed{\hat{\boldsymbol{h}}_i = \boldsymbol{F}\hat{\boldsymbol{h}}_{i-1} + \boldsymbol{g}_i(y(i) - \boldsymbol{x}_i^*\hat{\boldsymbol{h}}_{i-1})} \tag{4.12}$$

where

$$\boldsymbol{g}_i = \gamma(i)^{-1}\boldsymbol{F}\boldsymbol{P}_{i-1}\boldsymbol{x}_i \tag{4.13}$$

$$\gamma(i) = \sigma_n^2 + \boldsymbol{x}_i^*\boldsymbol{P}_{i-1}\boldsymbol{x}_i \tag{4.14}$$

$$\boldsymbol{P}_i = \boldsymbol{F}\boldsymbol{P}_{i-1}\boldsymbol{F}^* + \boldsymbol{G}\boldsymbol{R}_u\boldsymbol{G}^* - \gamma(i)\boldsymbol{g}_i\boldsymbol{g}_i^* \tag{4.15}$$

and $J_{(i)}$ is the cost function up to the time index i,

Here, we can also employ the backtracking algorithm introduced in Section (3.3.1) in the previous chapter to estimate the channel and detect the transmitted data blindly.

Table 4.1: Simulation and fading channel parameters

Parameter	Value
Packet length(N)	16
Channel length($L+1$)	4
Transmission frequency	2 GHz
Vehicle speed	50 and 200 km/hr
Symbol period	20 μs
Forgetting factor (λ)	0.999
Exponent of the channel decay profile (β)	0.2
The F-RLS parameter (η)	5

4.4 Simulation Results

In this section, we show simulation results for the performance of our blind equalization using Exponentially-Weighting RLS (EW-RLS), Extended RLS (E-RLS), and Fast RLS (F-RLS) algorithms. We investigate its performance in SISO system employing BPSK, 4QAM and 16QAM modulation over time variant channel IR generated according to the dynamical model in (4.3). We also study the effect of the time variation degree on the performance of the three methods. The parameters used in the simulation and generating the fading channel are shown in Table 4.1.

4.4.1 Performance of the three RLS algorithms

Here, we show simulation results for the performance of our blind algorithm using the three methods. We investigate its performance in SISO system employing BPSK, 4QAM and 16QAM modulation over time variant channel IR generated according to the dynamical model in (4.3) with $\alpha = 0.99995$ for a vehicle speed of 50 km/hr.

BER performance for BPSK modulated data

In Figures 4.1 and 4.2, we compare the new blind algorithm for BPSK modulated data over time variant channel using the three methods with $\alpha = 0.99995$ and 0.9951 respectively. We compare them also with the case of time invariant channel. As we see in Figure 4.1, the three methods work very close to the time invariant channel at low vehicle speed (50 km/hr corresponds to $\alpha = 0.99995$) while at high speed (200 km/hr corresponds to $\alpha = 0.99951$) only the F-RLS algorithm works better (see Figure 4.2).

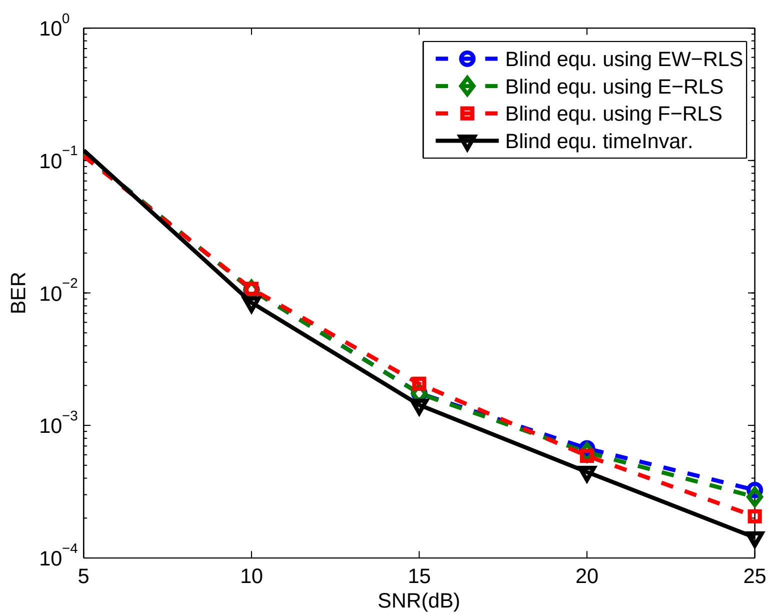

Figure 4.1: BER vs SNR for BPSK-SISO over time variant channel at low vehicle speed

BER performance for 4QAM modulated data

The same conclusion can be made for 4QAM modulation at high vehicle speed (200 km/hr corresponds to $\alpha = 0.99951$)(see Figure 4.3), where F-RLS algorithm shows

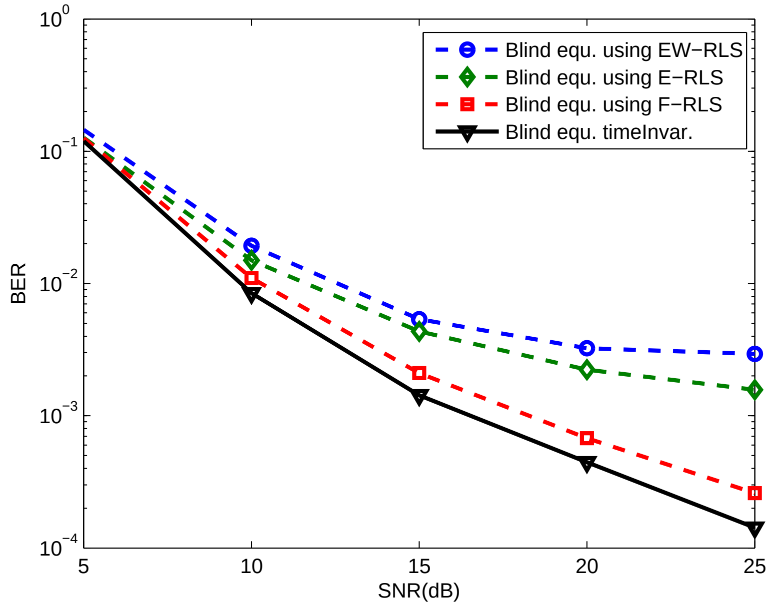

Figure 4.2: BER vs SNR for BPSK-SISO over time variant channel at high vehicle speed

favorable BER performance.

4.4.2 Effect of time variation

In this subsection, we test the performance of our receiver against different degrees of time variation. This is parameterized by α $(0 \leq \alpha \leq 1)$ with lower values of α indicating a faster time-variant channel. According to Table 4.1, the range of α is 99951 to 0.99995 for a vehicle speed decreasing from 200 km/hr to 50 km/hr, respectively.

For comparison, In Figures 4.4, 4.5, and 4.6, we show the BER curves for a system that employs BPSK data using the three methods EW-RLS, E-RLS and F-RLS to test its robustness against the time variation. It can be seen that the third method in Figure 4.6 has the best robust behavior when we change the time variant parameter

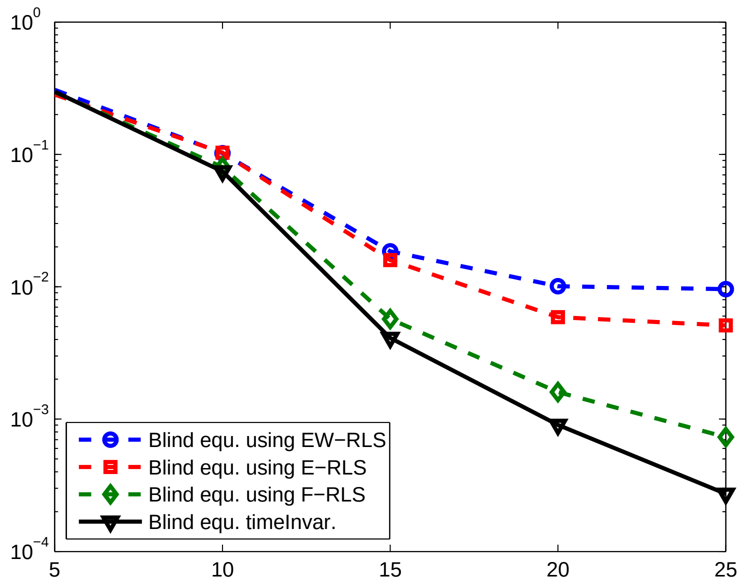

Figure 4.3: BER vs SNR for 4QAM-SISO over time variant channel at high vehicle speed

α from 0.99995 to 0.99951. Therefore, we are able to track the channel and capture time diversity at high vehicle speed.

4.5 Conclusion

In this chapter, we presented a blind algorithm for channel estimation and data recovery in linear convolution SISO transmission over frequency selective time-variant channels, where it varies form one data symbol to the next according to dynamical model. Three modification/extensions of the RLS algorithm were employed by the new blind algorithm which include the exponentially weighted RLS, the Fast RLS and the Extended RLS algorithm. The performance of the receiver by employing the three different implementations of the RLS was presented. Simulation results showed that

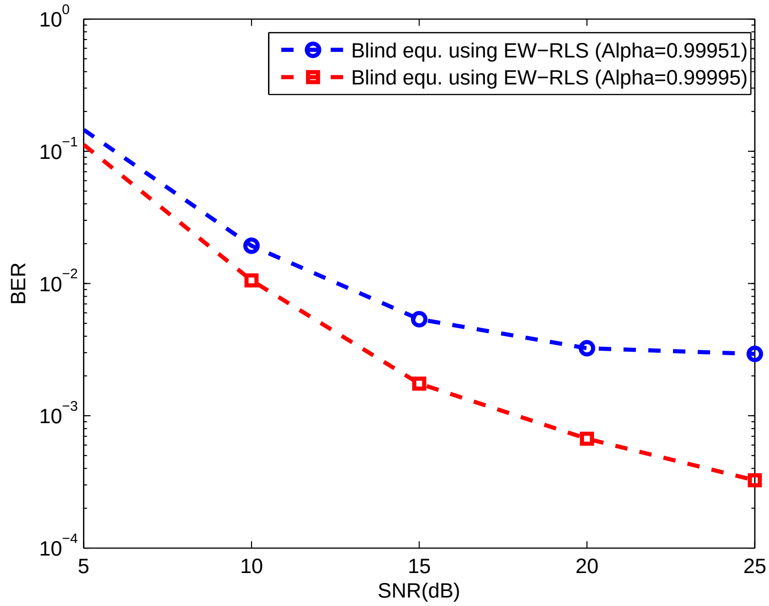

Figure 4.4: BER performance of EW-RLS method for BPSK over time variant channel

the Fast RLS algorithm outperforms the other two RLS algorithms.

We have also discussed the effect of the time variation parameters on the performance of the receiver. It was found that the receiver is able to estimate the channel effectively at high vehicle speed.

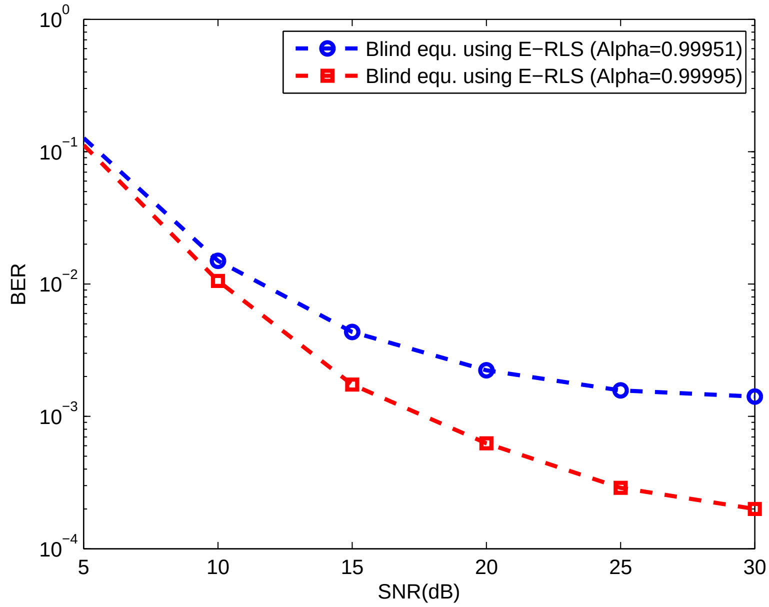

Figure 4.5: BER performance of E-RLS method for BPSK over time variant channel

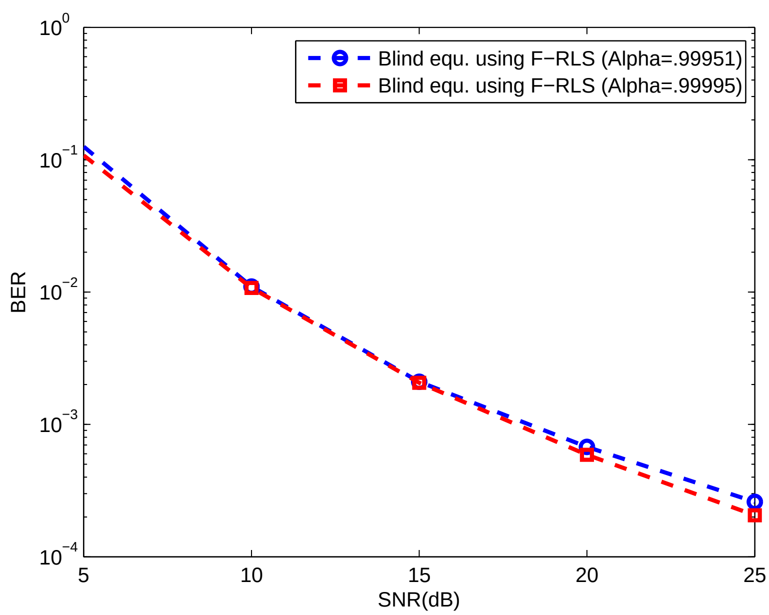

Figure 4.6: BER performance of F-RLS method for BPSK over time variant channel

CHAPTER 5

CONCLUSIONS AND FUTURE WORK

5.1 Concluding Remarks

This Thesis has considered blind algorithms for channel estimation and data recovery in SISO transmission. The first part of the Thesis presented a new blind algorithm for circular convolution SISO systems. We propose a low-complexity blind algorithm which achieves the exact ML data detection for OFDM wireless systems employing data with general constellations. The algorithm is able to recover the data from the output observations only. Simulation results showed the favorable performance of the algorithm for many constellations including the constant modulus (BPSK and 4QAM) and non-constant modulus (16QAM) constellations. To reduce the computational complexity involved in the blind algorithm, three methods were proposed; avoiding $\boldsymbol{P}_i$, avoiding $\boldsymbol{P}_i$ with ordering $\boldsymbol{A}_i$ and minimum cost methods. It was found that using the second method performed better than all other methods proposed. We can consider the minimum cost method as a pilot based estimation technique. Specifically, in this method, data is recovered by finding the constellation point that minimizing the cost function without backtracking giving a very low complexity.

The second part of Thesis presented the new blind algorithm for data detection in linear convolution SISO wireless systems employing data with general constellations. Simulation results showed the favorable performance of the algorithm for many constellations. It was found that using some pilots didn't add much improvement to the performance of the algorithm. We have also proposed approximate methods to reduce the complexity entailed in the blind algorithm. The structure of the regressors in the linear convolution SISO systems allowed us to use the Fast RLS algorithm which avoid the need for calculating the matrix $\boldsymbol{P}_i$ in the blind RLS algorithm and thus give lower complexity. As is evident from the simulation results, this approximate method perform quite close to the blind algorithm. A new equalization method (minimum cost method) was also proposed, when the receiver has perfect or estimated knowledge of channel.

The last part of Thesis considered a blind receiver design for linear convolution SISO transmission over time-variant channels. Some possible constraints on the channel (the finite delay spread, frequency and time correlation) and the data (the finite alphabet constraint) were utilized. Three modification/extensions of the RLS algorithm were employed by the new blind algorithm which include the Exponentially-Weighted RLS, Fast RLS and Extended RLS algorithms. The simulation results showed that the Fast RLS algorithm outperforms the other two RLS algorithms. We have also discussed the effect of the time variation parameters on the performance of the receiver, where the Fast RLS algorithm showed better robustness against the changing of the time variation parameters.

5.2 Future Work

5.2.1 General Time Variant Case for OFDM System

This Thesis deals with block fading channels in OFDM system (Chapter 2) i.e. the channel is assumed to be constant during the transmission of one OFDM symbol. It is more realistic to assume that the channel continuously varies with time which is a future research problem which can be build upon the findings in this Thesis. Specifically, we will assume that the channel varies within the OFDM symbol (resulting in intercarrier interference (ICI)) and use the various constraints used in this Thesis to perform channel estimation, ICI cancelation, and data detection.

5.2.2 Motivating the Constant Modulus Algorithm

Constant modulus algorithm (CMA) is a blind equalization method that uses the output observations only to detects the data without the need for any training sequence. Our blind algorithm does the same thing except that the CMA needs some time to converge while our algorithm can detects the data from the fist packet. So, with some modification on our algorithm we can motivate the CMA which does not have a basis of motivation.

5.2.3 Enhancing the Minimum Cost Method

The minimum cost method described in this Thesis does not consider any backtracking steps and thus gives a very low complexity, but it shows some sacrifice in the performance. So, a connection between this method and our blind backtracking method could enhance its performance. We can do a backtracking step to a flag point that has big difference between its cost function and an estimated value, this may help in enhancing the minimum cost method with some more calculations.

5.2.4 MIMO Channels Case

This Thesis deals with SISO channels, where the transmitter and the receiver use one antenna. Since, many wireless systems use more than one antenna for transmit and receive data, it is more practical to assume a Multiple-Input Multiple-Output (MIMO) channel which is a future research problem which can be build upon the findings in this Thesis. MIMO technology has attracted attention in wireless communications, because it offers significant increases in data throughput and link range without additional bandwidth or transmit power. We will assume that the transmitter and the receiver have more than one antenna and create a blind algorithm relying on our blind algorithm for both systems (linear and circular convolution) described in this Thesis.

REFERENCES

[1] Z. Wang and G. B. Giannakis, "Wireless multicarrier communications: Where Fourier meets Shannon," *IEEE Signal Proc. Mag.*, vol. 17, no. 3, pp. 29−48, May 2000.

[2] G. Stuber, J. Barry, S. Mclaughlin, Y. Li, M. Ingram, and T. Pratt, "Broadband MIMO-OFDM wireless communications," *Proc. IEEE*, vol. 92, no. 2, pp. 271−294, Feb. 2004.

[3] E. Chen, R. Tao, and X. Zhao, "Channel Equalization for OFDM System Based on the BP Neural Network," *Int. Conf. Signal Proc.*, vol. 3, Nov. 2006.

[4] T. Y. Al-Naffouri, "An EM-based forward-backward Kalman filter for the estimation of time-variant channels in OFDM," *IEEE Trans. Signal Proc.*, vol. 55, no. 7, pp. 3924−3930, Jul. 2007.

[5] N. Wang and S. D. Blostein, "Adaptive zero-padding OFDM over frequency-selective multipath channels," *EURASIP Journal on App. Signal Proc.*, pp. 1478−1488, Oct. 2004.

[6] X. Wang and R. Liu, "Adaptive channel estimation using cyclic prefix in multi-carrier modulation system," *IEEE Commun. Lett.*, vol. 3, no. 10, pp. 291−293, Oct. 1999.

[7] J. A. C. Bingham, "Multicarrier modulation for data transmission: An idea whose time has come," *IEEE Commun. Mag.*, vol. 28, no. 5, pp. 5−14, May 1990.

[8] G. B. Giannakis, "Filterbanks for blind channel identification and equalization," *IEEE Signal Proc. Lett.*, vol. 4, no. 6, pp. 184−187, Jun. 1997.

[9] B. Muquet, Z. Wang, G. B. Giannakis, M. de Courville, and P. Duhamel, "Cyclic prefixing or zero padding for wireless multicarrier transmissions?," *IEEE Trans. Commun.*, vol. 50, no. 12, pp. 2136−2148, Dec. 2002.

[10] B. Muquet, M. de Courville, G. B. Giannakis, Z. Wang, and P. Duhamel, "Reduced complexity equalizers for zero-padded OFDM transmissions," *IEEE Int. Conf. Acoust., Speech, and Signal Proc.*, vol. 5, pp. 2973−2976, Jun. 2000.

[11] J. van de Beek, O. Edfors, M. Sandell, S. K.Wilson, and P. O. Börjesson, "On channel estimation in OFDM systems," *IEEE Veh. Technol. Conf.*, vol. 2, pp. 815−819, Jul. 1995.

[12] O. Edfors, M. Sandell, J. van de Beek, K. S. Wilson, and P. O. Börjesson, "OFDM channel estimation by singular value decomposition," *IEEE Trans. Signal Proc.*, vol. 46, no. 7, pp. 931−939, Jul. 1998.

[13] Y. Li, L. J. Cimini, and N. R. Sollenberger, "Robust channel estimation for OFDM systems with rapid dispersive fading channels," *IEEE Trans. Commun.*, vol. 46, no. 7, pp. 902−915, Jul. 1998.

[14] M. Morelli and U. Mengali, "A comparison of pilot-aided channel estimation methods for OFDM systems," *IEEE Trans. Signal Proc.*, vol. 49, no. 12, pp. 3065−3073, Dec. 2001.

[15] M. Biguesh and A. B. Gershman, "MIMO channel estimation: optimal training and tradeoffs between estimation techniques," *IEEE Int. Conf. Commun.*, vol. 5, pp. 2658−2662, Jun. 2004.

[16] R. Negi and J. Cioffi, "Pilot tone selection for channel estimation in a mobile OFDM system," *IEEE Trans. Consumer Electr.*, vol. 44, no. 3, pp. 1122−1128, Aug. 1998.

[17] Y. Li, "Pilot-symbol-aided channel estimation for OFDM in wireless systems," *IEEE Vehicular Tech. Conf.*, vol. 2, pp. 1131−1135, May 1999.

[18] S. Ohno and G. B. Giannakis, "Optimal training and redundant precoding for block transmissions with application to wireless OFDM," *IEEE Trans. Commun.*, vol. 50, no. 12, pp. 2113−2123, Dec. 2002.

[19] M. Shin, H. Lee, and C. Lee, "Enhanced channel estimation technique for MIMO−OFDM systems," *IEEE Trans. Veh. Technol.*, vol. 53, no. 1, pp. 261−265, Jan. 2004.

[20] H. Minn and N. Al-Dhahir, "Optimal training signals for MIMO OFDM channel estimation," *IEEE Trans. Wireless Commun.*, vol. 5, no. 5, pp. 1158−1168, May 2006.

[21] I. Barhumi, G. Leus, and M. Moonen, "Optimal design for MIMO OFDM systems in mobile wireless channels," *IEEE Trans. Signal Proc.*, vol. 51, no. 6, pp. 1615−1624, Jun. 2003.

[22] F. Tufvesson and T. Maseng, "Pilot assisted channel estimation for OFDM in mobile cellular systems," *in Proc. IEEE Vehicular Tech. Conf.*, vol. 3, pp. 1639−1643, May 1997.

[23] Y. Li, N. Seshadri, and S. Ariyavisitakul, "Channel estimation for OFDM systems with transmitter diversity in mobile wireless channels," *IEEE J. Select. Areas Commun.*, vol. 17, no. 3, pp. 461−471, Mar. 1999.

[24] L. Tong and S. Perreau, "Multichannel blind identification: From subspace to maximum likelihood methods," *Proc. IEEE*, vol. 86, no. 10, pp. 1951−1968, Oct. 1998.

[25] R. W. Heath and G. B. Giannakis, "Exploiting input cyclostationarity for blind channel identification in OFDM systems," *IEEE Trans. Signal Proc.*, vol. 47, no. 3, pp. 848−856, Mar. 1999.

[26] B. Muquet, M. de Courville, P. Duhamel, and V. Buzenac, "A subspace based blind and semi-blind channel identification method for OFDM systems," *IEEE Workshop on Signal Proc. Advances in Wireless Comm.*, pp. 170−173, May 1999.

[27] A. P. Petropulu, R. Zhang, and R. Lin, "Blind OFDM channel estimation through simple linear precoding," *IEEE Trans. Wireless Commun.*, vol. 3, no. 2, pp. 647−655, Mar. 2004

[28] Z.Wang and G. B. Giannakis, "Linear precoded or coded OFDM against wireless channel fades?," *IEEE Workshop Sig. Proc. Adv. Wireless Commun.*, pp. 266−270, Mar. 2001

[29] W. Bai, C. He, L. Jiang, and S. China, "Blind channel estimation in MIMO-OFDM Systems," IEEE GLOBECOM, vol. 1, pp. 317−321, Nov. 2002.

[30] H. Bölcskei, R. W. Heath, and A. J. Paulraj, "Blind channel identification and equalization in OFDM-based multi-antenna systems," *IEEE Trans. Signal Proc.*, vol. 50, no. 1, pp. 96−109, Jan. 2002.

[31] G. A. Al-Rawi, T. Y. Al-Naffouri, A. Bahai, and J. Cioffi, "Exploiting error-control coding and cyclic-prefix in channel estimation for coded OFDM systems,"*IEEE Commun. Lett.*, vol. 7, no. 8, pp. 388−390, Aug. 2003.

[32] X. G. Doukopoulos and G.V. Moustakides, "Blind adaptive channel estimation in OFDM systems,"*IEEE Trans. Wireless Commun.*, vol. 5, no. 7, pp. 1716−1725, Jul. 2006.

[33] R. Zhang and W. Chen, "A mixture Kalman filter approach for blind OFDM channel estimation," *Asilomar Conf. on Signals, Syst., and Computers*, vol. 1, pp. 350−354, Nov. 2004.

[34] T. Petermann, S. Vogeler, K. Kammeyer, and D. Boss, “Blind turbo channel estimation in OFDM receivers,” *Asilomar Conf. on Signals, Syst., and Computers*, vol. 2, pp. 1489−1493, Nov. 2001.

[35] G. B. Giannakis and C. Tepedelenlioglu, “Direct blind equalizers of multiple FIR channels: a deterministic approach,” *IEEE Trans. Signal Proc.*, vol. 47, no. 1, pp. 62−74, January 1999.

[36] H. Wang, Y. Lin, and B. Chen, “Data-efficient blind OFDM channel estimation using receiver diversity,” *IEEE Trans. Signal Proc.*, vol. 51, no. 10, pp. 2613−2623, Oct. 2003.

[37] D. Xu and L. Yang, “Subspace-based blind channel estimation for STBC-OFDM,” *IEEE Int. Conf. on Acoust. Speech and Signal Proc.*, vol. 4, pp. IV − IV, May 2006.

[38] S. Roy and C. Li, “A subspace blind channel estimation method for OFDM systems without cyclic prefix,” *IEEE Trans. Wireless Commun.*, vol. 1, no. 4, pp. 572−579, Oct. 2002.

[39] S. Zhou, B. Muquet, and G. B. Giannakis, “Subspace-based (semi-) blind channel estimation for block precoded space-time OFDM,” *IEEE Trans. Signal Proc.*, vol. 50, no. 5, pp. 1215−1228, May 2002.

[40] B. Muquet, M. de Courville, and P. Duhamel, “Subspace-based blind and semi-blind channel estimation for OFDM systems,” *IEEE Trans. Signal Proc.*, vol. 50, no. 7, pp. 1699−1712, Jul. 2002.

[41] L. Chengyang and S. Roy, "Subspace-based blind channel estimation for OFDM by exploiting virtual carriers," *IEEE Trans. Wireless Commun.*, vol. 2, no. 1, pp. 141−150, Jan. 2003.

[42] C. Shin and E. J. Powers, "Blind channel estimation for MIMO-OFDM systems using virtual carriers," *IEEE GLOBECOM*, vol. 4, pp. 2465−2469, Dec. 2004.

[43] Y. Song, S. Roy, and L. A. Akers, "Joint blind estimation of channel and data symbols in OFDM," *IEEE Vehicular Tech. Conf.*, vol. 1, pp. 46−50, May 2000.

[44] C. Shin, R. W. Heath, and E. J. Powers, "Blind channel estimation for MIMO-OFDM Systems," *IEEE Trans. Vehicular Tech.*, vol. 56, no. 2, pp. 670−685, Mar. 2007.

[45] Z. Liu, G. B. Giannakis, A. Scaglione, and S. Barbarossa, "Decoding and equalization of unknown multipath channels based on block precoding and transmit-antenna diversity," *Asilomar Conf. on Signals, Syst., and Computers*, vol. 2, pp. 1557−1561, Oct. 1999.

[46] T. Kim and I. Eo, "Reliable blind channel estimation scheme based on cross-correlated cyclic prefix for OFDM system,"*Int. Conf. Adv. Commun. Technol.*, vol. 1, Feb. 2006.

[47] F. Gao and A. Nallanathan, "Blind channel estimation for OFDM systems via a general non-redundant precoding," *IEEE Int. Conf. Commun.*, vol. 10, pp. 4612−4617, Jun. 2006.

[48] F. Gao and A. Nallanathan, "Blind channel estimation for MIMO OFDM systems via nonredundant linear precoding," *IEEE Trans. Signal Proc.*, vol. 55, no. 2, pp. 784−789, Jan. 2007.

[49] R. Lin and A. P. Petropulu, "Linear precoding assisted blind channel estimation for OFDM systems," *IEEE Trans. Vehicular Tech.*, vol. 54, no. 3, pp. 983−995, May 2005.

[50] Y. Liang, H. Luo, and J. Huang, "Redundant precoding assisted blind channel estimation for OFDM systems," *Int. Conf. Signal Proc.*, vol. 3, 2006.

[51] M. Chang and Y. T. Su, "Blind and semiblind detections of OFDM signals in fading channels," *IEEE Trans. Commun.*, vol. 52, no. 5, pp. 744−754, May 2004.

[52] T. Y. Al-Naffouri, O. Awoniyi, O. Oteri, and A. Paulraj, "Receiver design for MIMO-OFDM transmission over time variant channels," *IEEE GLOBECOM*, vol. 4, pp. 2487−2492, Dec. 2004.

[53] B. Muquet and M. de Courville, "Blind and semi-blind channel identification methods using second order statistics for OFDM systems," *IEEE Int. Conf. on Acoust. Speech and Signal Proc.*, vol. 5, pp. 2745−2748, Mar. 1999.

[54] M. C. Necker and G. L. Stuber, "Totally blind channel estimation for OFDM on fast varying mobile radio channels," *IEEE Trans. Wireless Commun.*, vol.3, no. 5, pp. 1514−1525, Sep. 2004.

[55] K. Y. Ho and S. H. Leung, “A generalized semi-blind channel estimation for pilot-aided OFDM systems,” *IEEE Int. Symp. Circuits and Systems*, vol. 6, pp. 6086−6089, May 2005.

[56] S. Zhou, B. Muquet, and G. B. Giannakis, “Semi-blind channel estimation for block precoded space-time OFDM transmissions,” *Proceedings IEEE Signal Proc. Workshop on Statistical Signal Proc.*, pp. 381−384, Aug. 2001.

[57] T. Y. Al-Naffouri, D. Toumpakaris, A. Bahai and A. Paulraj, “An adaptive semi-blind algorithm for channel identification in OFDM,” *Asilomar Conf. on Signals, Syst., and Computers*, vol. 2, pp. 921−925, Nov. 2001.

[58] F. Yang and W. Ser, “Adaptive semi-blind channel estimation for OFDM systems,” *IEEE Veh. Technol. Conf.*, vol. 3, pp. 1773−1776, May 2004.

[59] T. Cui and C. Tellambura, “Joint data detection and channel estimation for OFDM systems,” *IEEE Trans. Commun.*, vol. 54, no.4, pp. 670−679, Apr. 2006.

[60] T. Cui and C. Tellambura, “Semi-blind channel estimation and data detection for OFDM systems over frequency-selective fading channels,” *IEEE Int. Conf. on Acoust. Speech and Signal Proc.*, vol. 3, pp. iii/597−iii/600, Mar. 2005.

[61] W. Yang, Y. Cai, and Y. Xun, “Semi-blind Channel estimation for OFDM Systems,” *IEEE Vehicular Tech. Conf.*, vol. 1, pp. 226−230, 2006.

[62] B. Yang, K. B. Letaief, R. S. Cheng, and C. Zhigang, “Channel estimation for OFDM transmission in multipath fading channels based on parametric channel modelling,” *IEEE Trans. Commun.*, vol. 49, no. 3, pp. 467−479, Mar. 2001.

[63] W. Kunji, Z. Jianhua, L. Chaojun, and H. Chen, "Semi-blind OFDM channel estimation using receiver diversity in the presence of virtual carriers," *Int. Conf. Commun. and Networking*, pp. 1−4, Oct. 2006.

[64] T. Y. Al-Naffouri, A. Bahai, and A. Paulraj, "An EM-based OFDM receiver for time-variant channels," *IEEE Globecom*, vol. 1, pp. 589−593, Nov. 2002.

[65] T. Y. Al-Naffouri, "Receiver design for MIMO OFDM transmission over time variant channels," *IEEE Workshop on Signal Proc. Advances in Wireless Comm.*, pp. 1−6, Jun. 2007.

[66] A. Paulraj, R. Nabar, and D. Gore, *Introduction to space time wireless communications.* Cambridge University Press, 2003.

[67] Z. Shengli and G. B. Giannakis, "Finite-alphabet based channel estimation for OFDM and related multicarrier systems," *IEEE Trans. Commun.*, vol. 49, no. 8, pp. 1402−1414, Aug. 2001.

[68] T. Y. Al-Naffouri, A. Bahai, and A. Paulraj, "Semi-blind channel identification and equalization in OFDM: an expectation-maximization approach," *IEEE Vehicular Tech. Conf.*, vol. 1, pp. 13−17, Sep. 2002.

[69] B. Lu, X. Wang, and Y. Li, "Iterative receivers for space-time block-coded OFDM systems in dispersive fading channels," *IEEE Trans. Wireless Commun.*, vol. 1, no. 2, pp. 213−225, Apr. 2002.

[70] Y. Li, C. N. Georghiades, and G. Huang, "Iterative maximum-likelihood sequence estimation for space-time coded systems," *IEEE Trans. Commun.*, vol. 49, no. 6, pp. 948−951, Jun. 2001.

[71] C. Aldana, E. de Carvalho, and J. M. Cioffi, "Channel estimation for multicarrier multiple input single output systems using the EM algorithm," *IEEE Trans. Signal Proc.*, vol. 51, no. 12, pp. 3280−3292, Dec. 2003.

[72] Y. Xie and C. N. Georghiades, "Two EM-type channel estimation algorithms for OFDM with transmitter diversity," *IEEE Trans. Commun.*, vol. 51, no. 1, pp. 106−115, Jan. 2003.

[73] C. Cozzo and B. L. Hughes, "Joint channel estimation and data detection in space-time communications," *IEEE Trans. Commun.*, vol. 51, no. 8, pp. 1266−1270, Aug. 2003.

[74] G. Stüber, *Principles of Mobile Communication.* Kluwer Academic, 2001.

[75] R.A. Iltis, "Joint estimation of PN code delay and multipath using the extended Kalman filter," *IEEE Trans. Commun.*, vol. 38, no. 10, pp. 1677−1685, Oct. 1990.

[76] C. Komninakis, C. Fragouli, A. H. Sayed, and R. Wesel, "Multi-input -input multi-output fading channel tracking and equalization using estimation," *IEEE Trans. Signal Proc.*, vol. 50, no. 5, pp. 5, pp. 1065−1076, May 2002.

[77] I. Kang, M. P. Fitz, and S. B. Gelfand, "Blind estimation of multipath channel parameters: a modal analysis approach," *IEEE Trans. Commun.*, vol. 47, no. 8, pp. 1140−1150, Aug. 1999.

[78] M.C. Vanderveen, A. -J. Van der Veen, and A. Paulraj, "Estimation of multipath parameters in wireless communications," *IEEE Trans. Signal Proc.*, vol. 46, no. 3, pp. 682−690, Mar. 1998.

[79] M. K. Tsatsanis, G. B. Giannakis, and G. Zhou, "Estimation and equalization of fading channels with random coefficients," *IEEE Int. Conf. on Acoust. Speech and Signal Proc.*, vol. 2, pp. 1093−1096, May 1996.

[80] T. Y. Al-Naffouri and A. Paulraj, "A forward-backward Kalman for the estimation of time-variant channels in OFDM," *IEEE Workshop on Signal Proc. Advances in Wireless Comm.*, pp. 670−674, Jun. 2005.

[81] J. Kennedy and R. Eberhart, "Particle swarm optimization,"*IEEE Int. Conf. on Neural Networks*, vol. 4, pp. 1942−1948, Nov. 1995.

[82] M. Clerc and J. Kennedy, "The particle swarm: Explosion, stability, and convergence in a multi-dimensional complex space," *IEEE Trans. Evol. Comput.*, no. 1, vol. 6, pp. 58−73, Feb. 2002.

[83] R. Mendes, J. Kennedy, and J. Neves, "The fully Informed Particle Swarm: Simpler May be Better," *IEEE Trans. Evol. Comput.*, vol 8, no.3, pp. 204−210, Jun. 2004.

[84] K. C. Sharman and G. D. McClurkin, "Genetic algorithms for maximum likelihood parameter estimation," *IEEE Int. Conf. on Acoust. Speech and Signal Proc.*, vol. 4, pp. 2716−2719, May 1989.

[85] S. Chen and Y. Wu, "Maximum likelihood joint channel and data estimation using genetic algorithms," *IEEE Trans. Signal Proc.*, vol. 46, no. 5, pp. 1469−1473, May 1998.

[86] A. Hjorungnes, D. Gesbert, and D. P. Palomar, "Unified theory of complex-valued matrix differentiation," *IEEE Int. Conf. on Acoust. Speech and Signal Proc.*, vol. 3, pp. III-345−III-348, Apr. 2007.

[87] J. R. Magnus and H. Neudecker, *Matrix Differential Calculus with Applications in Statistics and Econometrics.* John Wiley and Sons, Inc., 1999.

[88] H. Lutkepohl, *Handbook of Matrices.* John Wiley and Sons, Inc., 1996.

[89] K. B. Petersen and M. S. Pedersen, *The Matrix Cookbook.* Version 2006.

[90] A. Benveniste, M. Goursat, and G. Ruget, "Robust identification of a nonminimum phase system: Blind adjustment of a linear equalizer in data communications," *IEEE Trans. on Automatic Control*, vol. 25, no. 3, pp. 385−399, Jun. 1980.

[91] G. B. Giannakis and J. M. Mendel, "Identification of nonminimum phase systems using higher order statistics," *IEEE Trans. on Acoust., Speech, and Signal Proc.*, vol. 37, no. 3, pp. 360−377, Mar. 1989.

[92] Ali H. Sayed, *Fundamentals of Adaptive Filtering.* John Wiley and Sons, Inc., 2003.

[93] T. Kailath, A. H. Sayed, and B. Hassibi, *Linear Estimation.* Prentice Hall, 2000.

[94] S. M. Alamouti, "A simple transmit diversity technique for wireless communications," *IEEE J. Select. Areas Commun.*, vol. 16, pp. 1451−1458, Oct. 1998.

[95] E. Larsson and P. Stoica, *Space-Time Block Coding for Wireless Communications.* Cambridge University Press, 2003.

[96] T. Y. Al-Naffouri, Adaptive Algorithms for Wireless Channel Estimation: Transient Analysis and Semi-Blind Design, Stanford University, Jan. 2005.

[97] Weiyu Xu, Mihailo Stojnic and Babak Hassibi, "Low-Complexity Blind Maximum-Likelihood detection for SIMO systems with general constellation," IEEE International conference on Acoustics Speech and Signal Processing (ICASSP), vol. 1 ,PP. 2817-2820, Apr. 2008.

[98] Tareq Y. Al-Naffouri and Ahmed Abdul Quadeer, "Blind Maximum-Likelihood Data Recovery in OFDM," IEEE International Conference on Acoustics Speech and Signal Processing (ICASSP), vol. 1, pp. 2829-2832, Apr. 2008.

[99] Pei Chen and Hisashi Kobayashi, "Maximum Likelihood Channel Estimation and Signal Detection for OFDM Systems," IEEE International Conference on Communications (ICC), vol. 3, pp.1640-1645, Feb. 2002.

[100] R. W. Heath Jr. and G. B. Giannakis, "Exploiting input cyclostationarity for blind channel identiffcation in OFDM systems," IEEE Trans. Sig. Proc., vol. 47, no. 3, pp.848-856, Mar. 1999.

Vitae

- Ala$'$ Ahmad Dahman.
- Nationality : Palestinian
- Born in Hebron, Palestine on May 24^{th}, 1981.
- Received Bachelor of Engineering (BE.) degree in Electrical Engineering from Palestine Polytechnic University, Hebron, Palestine in June 2004.
- Joined King Fahd University of Petroleum & Minerals in September 2007.
- Present Address: KFUPM Campus - Dhahran - Saudi Arabia.
- Permanent Address: Wad AlHariya Street - Hebron - Palestine.
- Email: dahman@kfupm.edu.sa, dahmanalaa@gmail.com
- Mobile: 00966-555-786-425